| | |
|---|---|
| Title | 含浸法を利用したポリプロピレンナノコンポジット中への無機ネットワーク構造の合成 |
| Author(s) | 金子，慧 |
| Citation | |
| Issue Date | 2016-03 |
| Type | Thesis or Dissertation |
| Text version | ETD |
| URL | http://hdl.handle.net/10119/13527 |
| Rights | |
| Description | Supervisor:寺野　稔，マテリアルサイエンス研究科，博士 |

# Synthesis of Inorganic Network Structure in Polypropylene Nanocomposite Prepared by Impregnation Method

KEI KANEKO

Japan Advanced Institute of Science and Technology

# Synthesis of Inorganic Network Structure in Polypropylene Nanocomposite Prepared by Impregnation Method

**by**

**Kei Kaneko**

Japan Advanced Institute of Science and Technology
1-1 Asahidai, Nomi, Ishikawa, 923-1292, Japan

**Supervisor: Professor Minoru Terano**

School of Materials Science
Japan Advanced Institute of Science and Technology

March 2016

Referee-in-chief: **Professor Dr. Minoru Terano**

*Japan Advanced Institute of Science and Technology*

Referees: **Professor Dr. Masayuki Yamaguchi**

*Japan Advanced Institute of Science and Technology*

**Associate Professor Dr. Tatsuo Kaneko**

*Japan Advanced Institute of Science and Technology*

**Associate Professor Dr. Toshiaki Taniike**

*Japan Advanced Institute of Science and Technology*

**Professor Dr. Koh-hei Nitta**

*Kanazawa University*

# Synthesis of Inorganic Network Structure in Polypropylene Nanocomposite Prepared by ImpregnationMethod

s1340003: Kei Kaneko

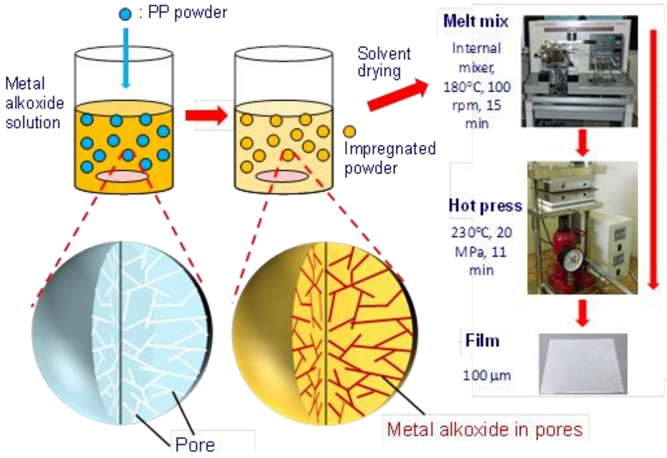

Polypropylene (PP) is one of the most widely used polyolefin due to good mechanical properties, high processability, low environmental load and high chemical resistance. PP-based nanocomposites have attracted particularly large expectation owing to its high demand in the market. However, it is difficult to achieve good dispersion of polar fillers in the nonpolar PP matrix. Method for overcoming this problem is addition of compatibilizer such as maleic anhydride grafted PP, organic modification filler surface, and using in-situ sol gel method.

In this research is to develop a more versatile strategy for the large-scale fabrication of nanosized metal oxide networks in the PP matrix. We use impregnation method for the pretreatment. It considered that precursor dissolved in a solvent impregnate for polymer and can prepare PP/common ceramics nanocomposites.

In this study, PP/metal oxide nanocomposites were prepared through the impregnation of PP amorphous part with metal alkoxide and subsequent sol-gel reaction. A new approach for preparing better PP nanocomposites is to apply the sol-gel technique. We tried to impregnation and sol-gel reaction of metal alkoxide in porosity of PP reactor powder, which have a large number of pores derived by the structure of the catalyst. It leads to the formation of an inorganic network throughout the polymer matrix. It was attempted to develop more versatile strategy for the large-scale fabrication of nanosized metal oxide network in the PP matrix. In chapter2, the metal oxide particle was prepared with the impregnation time of 9 h makes homogenously dispersed and formed small aggregates in the matrix. It was suggested that long time of impregnation method impregnate the precursor into pores of PP powder surface. It considered that long period of time reach the impregnation equilibrium.

In chapter 3, PP/$Al_2O_3$ nanocomposites was prepared using impregnation method, where a precursor dissolved in solvent was impregnated into pores of PP reactor powder prior to sol-gel reaction. Thermal conductivity may be achieved by introducing a network structure of $Al_2O_3$ within polymer matrix. The thermal conductivity was improved by the method, owing to the formation of $Al_2O_3$ filler network. Further, combination of impregnation and sol-gel methods with nanoparticle was found to be quite effective for achieving the high thermal conductivity of PP nanocomposites.

Novel design of metal oxide network in polypropylene using sol-gel method using impregnation method achieved and the development is expected to expand both academic and industrial area.

Key Words: Polypropylene, Nanocomposite, Sol-gel method, Impregnation, Network structure

# Contents

Chapter 4. Influences of Mechanical Properties on Polyethylene-based Nanocomposites using Polyethylene-grafted Nanosilica Nanoparticles

Chapter 5. The Development of High-Performance and Practical Nanocomposites using In-Situ Polypropylene Grafting Reaction

Chapter 6. General Conclusion

# Chapter 1

# General Introduction

## *1.1. Polypropylene*

### *1.1.1. Background*

Before 1950, polypropylene (PP) was low-molecular weight branched oil, which did not show an attractive property. Ziegler-Natta catalyst was discovered, however, and polypropylene containing 30-40% of isotactic polypropylene was synthesized for the first time by Natta in 1954 using $TiCl_4/AlR_3$ catalyst[1-3]. Since then hitherto, various researches, such as researches on very complicated Ziegler-Natta catalyst active spot and development of high-performance catalysts, have been conducted aiming at higher catalytic activity and higher stereoregularity. Now, supported Ziegler-Natta catalyst shows very higher catalytic activity than ever, and among all, $MgCl_2$ supported catalyst shows significantly high activity. With alkylaluminium compound combined with Lewis base called an external donor and used as promoter, this supported Ziegler-Natta catalyst enables polypropylene containing higher isotactic polypropylene (95-99%) to be synthesized. And now, about 2.86 million ton of polypropylene a year is produced in Japan[4]. Production of polypropylene, one of five multi-purpose resins, tends to increase recently more than low-density polyethylene, high-density polyethylene, polystyrene, and polyvinyl chloride. This is because polypropylene has many good properties, such as good molding processing properties and heat resistance, low price, little environmental load since it produces carbon dioxide and water when it burns, light weight among plastics, specific gravity of about 0.9, lighter than water by about 10%, and high strength. Since it has melting point of as high as 160°C and good chemical resistance, it can be sterilized with hot water and steam. By utilizing these properties, it is used in various fields and applications, such as medical syringes, food packaging films, automobile bumpers, battery containers, and interiors[5].

### *1.1.2. Development of Ziegler-Natta Catalysts for propylene polymerization*

Three main types of catalysts are used in olefin polymerization: Ziegler-Natta, Phillips and metallocenes. Phillips catalyst, which chromium oxide ($CrO_X$) is impregnated on a silica support [6], is industrial PE catalyst, differing from the ZN catalysts in that they are activated in situ by ethylene during the polymerization (*i.e.* no cocatalyst is present). Metallocene catalyst, which are organometallic coordination compounds having one or two cyclopentadienyl rings or substituted cyclopentadienyl rings bound to a central transition metal atom and activated by methylaluminoxane [7], become recently used for commercial HDPE production, but is still limited for PP production. ZN catalyst is most widely used for Industrial PO production, of 99% of polypropylene (PP) and 50% of polyethylene (HDPE), and has been used in numerous applications. The development of ZN catalysts has long history along with the industrial demands. It is widely accepted that five different generations of ZN catalysts exist. As the development of catalyst chemistry has continued, the polymer morphology, properties and reactivity have been improved.

The $TiCl_3/AlEt_2Cl$ catalyst used in the earlier industrial processes for PP manufacturing, showed low productivities (only 1 kg per g of catalyst) and stereo-specificity (the boiling-heptane-insoluble fractions was only 90%). Thus, both separation of the atactic polymer fraction and removal of the polluting catalytic residues (inactive titanium salt) were required [8], increasing the complexity and cost of the production process. Enormous efforts were invested to simplify the production process in order to dispense with the extra facilities and energy for removing the undesirable components. It is evident that the catalyst performance is the real core of the problem, which explains why a great deal of effort was devoted to the characterization and the comprehension of the catalytic system.

As a result of the preparation method used, only a small fraction of total Ti atoms (located at the surface of the heterogeneous $TiCl_3$ catalyst) were accessible to the reducing agent (Al-alkyl) for making active polymerization sites [9,10]: i.e. only one titanium site out of 1000 participated in the catalytic process. The catalytic productivity had to be increased: since polymerization takes place on the catalyst surface, it is natural that much effort was devoted to increasing the accessibility of Ti atoms. Two main approaches were tested: (i) reducing the size of the catalyst microparticle (crystallites), and (ii) supporting Ti compounds on the surface of inorganic materials with a chemical reaction.

The first route leads us to the second generation of $TiCl_3$ catalysts. Several research efforts were carried out to acquire a basic understanding of the catalytic system (on the formation of active sites and the reaction leading to their structure), making the synthesis of an improved $TiCl_3$ catalyst possible. The new supported catalyst possessed a nearly spherical shape, a mean size in the range 20-40 μm and a narrow particle size distribution (PSD). This catalyst consists of aggregates of subparticles made of very small primary crystallites (50-100 Å). The particle porosity is mainly due to micro-pores ($d_p < 200$ Å) inside subparticles. Compared with the earlier generation, this catalyst is characterized by a lower primary crystallite size, a much higher surface area, and by the presence of an Al-alkyl reductive agent (e.g. DEAC) and a Lewis base (e.g. benzoic acid esters, alkoxysilane) that made it possible to increase both productivity by a factor of up to 10 in the industrial process and, in the case of PP, isotacticity of I.I. = 95%.

In the 1960s, an essential innovation was achieved by two research groups (Montedison, Italy and Mitsui Petrochemcal Industries, Japan) with the development of the third generation of catalyst. These are based on the use of conventional high surface inorganic supports, e.g. silica, alumina, Mg-hydroxides or Mg-hydroxychlorides, and bear several surface functional group (mainly –OH) able to chemically anchor the transition metal compounds. Because of their insufficiently low activity for PE and PP polymerization, the development efforts naturally continued until the discovery of the catalysts based on "activated" $MgCl_2$, highly active both for PE and PP [11]. But, owing to their very low stereo-specificity (I.I. $< 50\%$), their use was initially limited to PE. One must not forget that, not only the enhancement of catalyst activity but also the control of the catalyst stereo-specificity are of great importance especially in the case of PP polymerization.

An improved version was therefore developed, essentially composed of $TiCl_4$ supported on $MgCl_2$, with trialkyl-aluminium (TEA) as a cocatalyst and an efficient combination of Lewis bases as internal donors (additives in the solid catalyst) and/or external donors (additives in the polymerization system) [12]. This new $MgCl_2$ supported donor-modified catalyst system is the root of a large family of efficient catalysts.

Since the early 1970s, in order to generate the "ideal" catalyst, the research efforts focused not only on more efficient routes for catalysis synthesis, but, to an even greater extent, on the clarification of unanswered questions in the field of catalysis chemistry. Particular efforts were made on understanding the mechanisms of olefin polymerization, the nature of the active sites, the deactivation reactions related to the variation of oxidations state of titanium species, the effect of the carrier and the Lewis bases on the polymer properties, etc. As a result, in the early 1980s, the discovery of the efficient combination of alkylphtalates as internal donors and alkoxysilanes (or silyl-ethers) as external donors, and the emergence of a new type of electron donor, the 1,3-diethers (used only as an internal compound and not requiring any external donor), in the second half of the 1980s, gave rise to extremely efficient fourth and fifth generation catalyst systems (productivity > 2400 kg-PP/g-Ti, I.I. > 98%) [13]. Comparisons of the performance achievable with the different catalyst generations have been often reported.

### *1.1.3. Crystalline structures of PP*

Polypropylene homopolymer is essentially semi-crystalline. All semi-crystalline polymers exhibit hierarchical structure of a characteristic scale as shown in Figure 1.1. Macroscopic morphology is observed in a visible scale (i.e. millimeter). This scale corresponds to the gross shape and skin-core structure of a reactor particle, for example. Spherocrystal structure is observed in a finer scale, which is 1-50 μm in order. Sphero-crystalline consists of lamella crystalline that consists of polymer chains.

The stereoregularity of polymer chains of PP is classified largely into three categories. Figure 1.2 shows three categories of polymer chains of PP. In isotactic chains, methyl groups always have the same configuration to the polymer skeleton. In syndiotactic chains, methyl groups have alternate configuration to the polymer skeleton, and in atactic chains, methyl groups have no specific regularity.

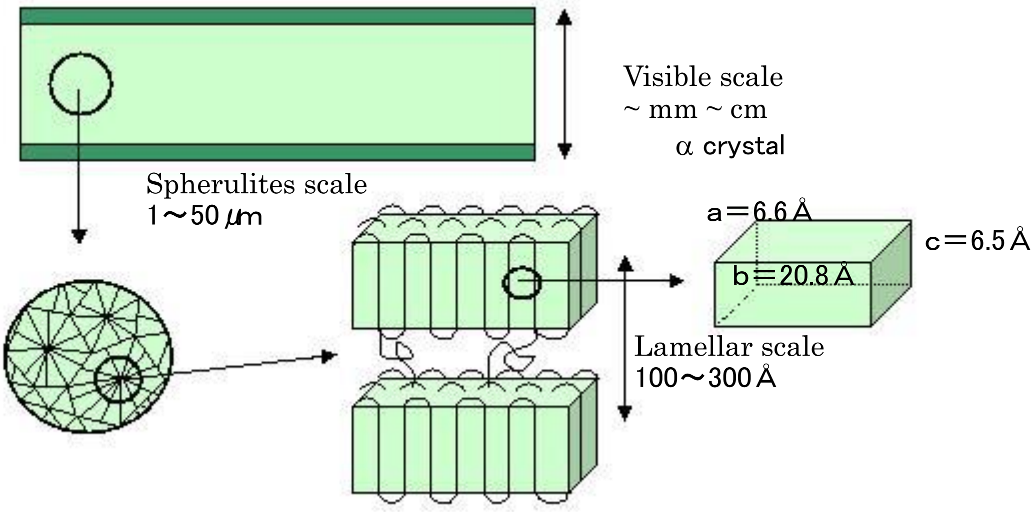

Figure 1.1. Higher order structure of PP

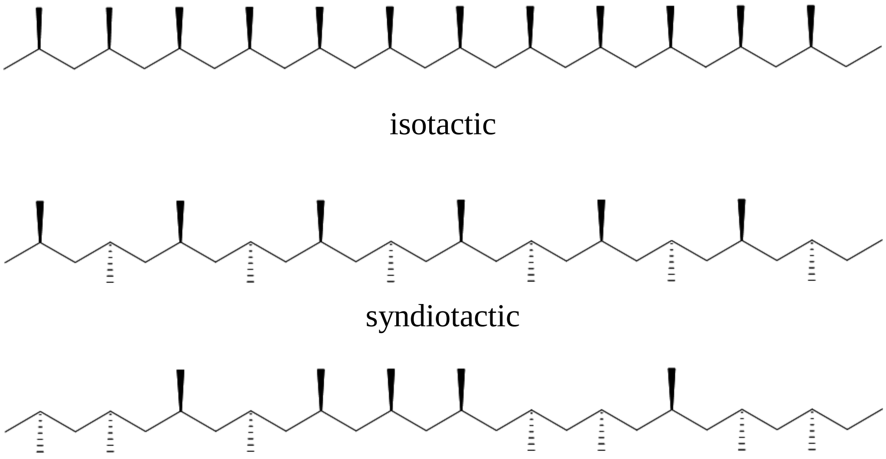

atactic

Figure 1.2. Stereo configuration of polypropylene.

Although usual crystallization condition lead to the formation of α form in iPP, other crystalline structure, β and γ forms, are also formed depending on the conditions. Determination of the crystal unit cell of the β form in iPP based on WAXD measurements showed two reflections at *d*-spacing of 0.553 nm and 0.417 nm [14]. These two peaks are believed to fit into a hexagonal lattice with $a$ = 1.274 (or 0.636) nm, $c$ = 0.635 nm, γ = 120° and α =β = 90°. Therefore, these two reflections should be (100) and (101) reflections [15]. Another report proposed that the hexagonal lattice should be a = 1.908 nm, c = 0.649 nm, γ = 120° and α = β = 90°, thus assigning (300) and (301) reflections to these two *d*-spacing. The crystallographic density was calculated to be 0.921 g/cm$^3$ [16]. Other reports also suggested that this metastable crystal form must be recognized as a trigonal lattice, which could also be grouped as a subdivision of the hexagonal lattice system. The β form in iPP is thermodynamically less stable than the α form in normal crystallization conditions. Crystallization in a temperature gradient or the use of selective nucleating agents is the typical way to get mostly β form PP in the materials. The β form in iPP can be transformed into the α form by drawing or by recrystallization at the temperature range near melting point of the bulk samples. The thermodynamic properties of the β form have not been studied compared to those of α form. The $T_m°$ was extrapolated by several research groups, and values varied from 170°C to 200°C [17-

19].

The crystal structure and unit cell geometry of the γ form in iPP are known only approximately, but strongly resemblance to those of α form are reported. The proposed triclinic unit cell parameters are *a* = 0.654 nm, *b* = 2.14 nm, *c*= 0.650 nm, α = 89°, β = 99.6° and γ = 99° [20]. The crystallographic density was 0.954 g/cm$^3$. This unit cell appears to result from the monoclinic α form by a simple shear along *a* axis [20]. The γ form often observed in low molecular weight iPP or in iPP synthesized by the metallocene catalyst [21, 22]. However, in most cases the one may find co-existence of the α and γ forms in the crystals [23]. The γ form is known to nucleate on crystals of the α form, but the crystallographic relationship between these two forms is still not fully understood, even resent studies by Lotz, Graff and Wittmann plausibly explained the relation ships [24]. When the γ form crystals are nucleated on the α form, the contact planes of both the α and γ forms are (010). They have their *b** and *c* axes parallel. The γ form crystal overgrowth reflects the mirror symmetry that exists at the molecular level in the α form crystals. Since the γ form crystals have their lamellar surface inclined to the chain axis, while in the α form crystals it is perpendicular to it, the γ form crystals grown on the α form crystals appear to branch. The thermodynamic properties of the γ form are not well determined.

### *1.2. Polypropylene composite*

Although PP resin is a material having good flow property, chemical resistance, weather resistance, and economical efficiency, its strength, stiffness, and impact resistance are not enough. Various kinetic properties have been improved in response to applications by adding inorganic filler and different polymer to PP. In many cases, compounding method can respond to market needs through a quicker and cheaper route than new reactor-based polymer development, and is therefore used widely. Since PP has good specific properties such as high melting point, chemical resistance, and low specific gravity, it is one of the most important commercially available resins. Since PP can be compounded with large quantity of filler, reinforcing agent, and different polymer, it has high diversity. Blending makes the range of physical properties of PP wider, and materials having physical properties suited to specific applications can be produced. In addition, many of these physical property improvements are realized with the cost advantages of PP sustained. As a result, PP compound products have grown up, and occupy important parts in the PP industry.

PP in which inorganic materials have been filled has good performance and recycling efficiency, and diversity of design processing. Filler compounded PP has not only a wide range of physical properties and advantageous economical efficiency but also a wide range of molding suited to many applications requiring sheet extrusion, profile extrusion, and hot molding properties. By selecting suitable filler, PP grade, and compounding technique, products exhibiting physical properties equal to some engineering plastics can be designed. For these reasons, inorganic materials are used not only to reduce polymer consumption and cost but also to improve performance. As a result, a considerable number of filler compounded PP grades has been developed and used effectively for various applications in the markets of automobile, architecture, construction, electronics, sporting goods, and others.

### *1.3. Characteristics of inorganic filler*

Filler is a generic name of inert additives used for the purpose of reinforcement of materials, improvement of various properties, and cost saving. Effect of filler depends largely on type and shape of filler to be added, and filler is classified by composition (oxides, hydroxides, salts, nitrides, carbons, metals, etc.), by shape (needle, plate, ball, particle, etc.), and by function (conductivity, thermoelectricity, flame resistance, gas barrier, etc.) Combination of them changes kinetic properties, thermal properties, electrical properties, and optical properties.

Filler essentially means powders and particles to be filled in rubber and plastic. The "1st generation" filler was used as an extender when synthetic resins were invented, and crushed naturally occurring ores such as calcium carbonate and clay were used.

In the "2nd generation", powder, fiber, needle, and plate filler appeared, and artificial filler such as potassium titanate was also used to reinforce kinetic and thermal properties of plastic.

In the "3rd generation", functional filler providing rubber and plastic with various functions appeared. To bring out performance of filler, control or processing of shape and particle size was provided.

And as the "4th generation", nano-sized ultra-fine particle filler appeared recently. With improvement of kinetic properties and addition of functionality exceeding the 3rd generation, nano-filler is expected to contribute to high-performance or high value addition as a composite material in the 21st century and attracts attention in the high technology field.

The basic role of filler for polymeric materials has been used for many years. To reduce cost, filler cheaper than matrix polymer is filled, and it has not only economic effect due to cost reduction but also an important role to be used for multi-purpose resins to substitute super engineering plastics.

This role includes improvement of properties of polymeric materials and addition of functionality to them. Improvement of physical properties is important in improvement of performance of polymeric materials to improve kinetic properties and thermal properties of them. Addition of functionality includes addition of special functions polymeric materials do not have essentially, or reinforcement and improvement of functions, which is important in high-performance or high value addition of polymeric materials.

In addition, filler also has effects of improvement of workability; such as control of viscosity, flow property, and curing time, stability of molding dimension, prevention of contamination of dies, acceleration of die-release of polymeric materials at processing, suppression of orientation of fiber, and dispersion auxiliary agents for various additives; and plays a wide role to improve workability of polymeric materials. Like this, inorganic filler has large potential and expectation to polymeric materials.

### *1.4. Polymer Based Nanocomposites*

Nano-composite is compounding technique using nanometer particles as filler. Filler is a generic name of inert additives for matrix polymer; since blending of low price filler in matrix improves kinetic properties and thermal properties, it has played an important role in cost reduction and high-performance of synthetic resin products for many years. Nano-composite is intended to improve further mechanical performance of polymer matrix by micronizing filler to molecular size. Typical nano-size filler (nano-filler) includes laminated clay compound montmorillonite and silica. Polymer composite is intended to improve mainly kinetic properties and thermal properties by dispersing filler in matrix; to realize these, control of interfacial tension between filler and matrix has been studied. A method of using a compatibility accelerator and a method of providing organic modification on the surface of particles have been developed so far.

### *1.4.1. Polypropylene Based Nanocomposites*

Nano-composite with PP used as matrix is of low preparation cost, improves physical properties significantly by addition of particles, and is very valuable materials. Since polar inorganic filler is not compatible with nonpolar PP, however, filler does not disperse, forms aggregate, and causes deterioration of physical properties. Therefore, surface modification of inorganic filler and alteration or modification of PP are required. Silica nano-particle, one of inorganic fillers, has many reactive functional groups on its surface, which makes modification easy.

To solve problems with nano-composite, various researches have been conducted on PP/$SiO_2$ system. One is a method with emphasis on high dispersibility of particles using a compatibility accelerator such as maleic anhydride modified PP. Another is a method of modifying the surface of particles with short-chained alkyl using a silane coupling agent.

Researches using ceramics filler to add functions to polymer have been conducted. Nano-composite with ceramics filler having good functional properties added attracts attention in various fields, and high-performance and multifunction by polymer/ceramics compounding has been required. Chakrabarti, et al. added zinc oxide to PVP to provide antibacterial activity and properties as an active oxygen sensor. Hu, et al. added tin oxide to polyaniline to improve capacitor properties. Researches on addition of functions to polymer using filler have also been conducted for PP; Marks, et al. used in-situ polymerization method by which propylene was polymerized with barium titanate ($BaTiO_3$) filler to improve the dielectric constant. To provide antibacterial activity, Cassagnau, et al. used in-situ sol-gel method by which $TiO_2$ precursor was sol-gel reacted in PP at kneading to produce filler.

Sol-gel method is a method of synthesizing ceramics filler in polymer by hydrolysis and dehydration condensation of filler precursor, and it can synthesize inorganic network filler in polymer. As preparation method of nano-composite by sol-gel method, solution blend and a method of impregnating precursor in polymer are used widely. On the other hand, since PP does not dissolve in common solvent and impregnation of precursor is difficult, precursor is impregnated in film at melting kneading with sol-gel reaction combined to produce nano-composite. As an example, Sun, et al. used supercritical carbon dioxide to impregnate silica precursor in PP film and improve dispersibility of filler by sol-gel reaction in the film.

### *1.4.2. Network formation*

Network structure can provide a new function of the polymer material and an inorganic material. Electrical and thermal properties can be produced by introducing a three-dimensional network of the inorganic filler within the polymer matrix. The importance of inorganic network for the origin of the potential new functions of the in the polymer, has been well documented in the literature [25-27]. Harrison et al. found that the networks of single-walled carbon nanotube (SWNT) in polyimide enhanced the electrical conductivity by many orders of magnitude at a nanotube loading of only 0.1 vol% [25]. Du et al. reported that the addition of SWNT in a poly(methyl methacrylate) (PMMA) matrix brought about great improvements in the thermal stability and the fire retardancy, where the networks of SWNT significantly reduced the heat release rate of

PMMA. Sun et al. synthesized nanosized silica networks distributed uniformly in a polypropylene (PP) matrix and thereby obtained significant increase in the mechanical properties [27]. Cassagnau et al. studied the morphology and viscoelasticity of PP/$TiO_2$ nanocomposite [28]. Alteration of the terminal relaxation into a solid-like behavior results from the formation of an aggregate network.

### *1.5. Thermal conductivity*

The dispersion of thermally conductive fillers in a polymer matrix can result in an increase in thermal conductivity of the polymer. Owing to the demands in several area, the dissipation of heat generated has attracted more attention and is considered as a critical issue to be resolved. To solve the heat dissipation problem, ceramic fillers, such as alumina ($Al_2O_3$)[29-32], silica ($SiO_2$)[33,34], silicone carbide (SiC)[35], silicon nitride ($Si_3N_4$)[36-38], aluminum nitride (AlN)[39-44], and boron nitride (BN)[45-52], were used as the thermal conductive materials embedded in a polymer matrix. The heat transport mechanism of the nonmetals is explained by the flow of phonons or lattice vibration energy. Hence, the polymer/ceramics composites form a thermally conductive path or network, which can decrease the heat generated by the phonon scattering in the polymer matrix. The conventional method to fabricate the thermally conductive composites is to use loading of thermally conductive fillers[41-45, 53,54] to form a thermally conductive network.

### 1.6. Objective

By using polymerized PP powder having fine pores on its surface and immersing PP powder in solution in which metal oxide precursor is dissolved, the metal oxide precursor can enter fine pores on the surface of powder. In this research, various metal oxide precursors are dispersed in PP powder by impregnation method, and then nano-composite with metal oxide filler dispersed in PP by thermal sol-gel reaction is produced.

### 1.7. References

[1] Ziegler, K., Holzkamp, E., Breil, H., Martin, H. *Angew. Chem.* **67**, 541 (1955).

[2] Natta, G., Pino, P., Corradini, P., Danusso, F., Mantica, E., Mazzanti, G., Moraglio, G. *J. Am. Chem. Soc.* **77**, 1708 (1955).

[3] Galli, P., Haylock, J. C. *Makromol. Chem*, Macromol. Symp. **63,** 19 (1992).

[4] Moore Jr., E. P. "Chapter 6: End-Use Properties", In: *Polypropylene Handbook*, Moore Jr., E. P. Ed., Carl Hanser Verlag, Munich, p237 (1996).

[5] Galli, P., In: *International Union of Pure and Applied Chemistry, Structural Order in*

*Polymers*, Giardelli, F., Giusti, P., Eds., Pergamon Press, London, 63. (1981).

[6] Esso Res. & Eng. Co., *US Pat.* 3, 128, 252 (1964).

[7] Yamaguchi, K., *Kobunshi.* **30**, 199. (1981).

[8] Goto, K., Ishii, K., Kataoka, T., Terano, M. *Fine Chemical*, **23**, 32 (1994).

[9] Natta, G,. Pasquon, I. *Adv. Catal.* **11**, 1 (1959).

[10] a) Solvay & Cie *Ger. Pat.* 2, 213, 086 (1972).

b) Solvay & Cie *US Pat.* 3, 7, 69, 233 (1973).

[11] Bernard, A., Fiasse, B. In: *Catalytic Olefin Polymerization*, Keii, T., Soga, K., Eds., Kodansha-EIsevier, p405 (1990).

[12] Montedison S. p. A *Brit. Pat.* 1, 286, 867 (1968).

[13] AIbizatti, E., Giannini, U., Collina, G., Noristi, L., Resconi, L. "Catalyst and polymerizations", In: *polypropylene Handbook*, Moore Jr., E. P. Ed., Hanser Publishers, Munich. Vienna, New York, pp11-110 (1996).

[14] Keith, H.D., Padden, Jr, F.J., *et al. J. Appli. Phys.* **30**, 1485 (1959).

[15] Addink, E.J., Bientema, J. *Polymer* **2**, 185 (1961).

[16] Samuels, R. J., Yee, R. Y. *Journal of Polymer Science, Part A* **10**, 385 (1972).

[17] Lovinger, A.J., Chua, J.O., Gryte, C.C. *J. Polym. Sci. Polym. Phys.* **15**, 641 (1977).

[18] Shi, G.Y., Huang, B., Zheng, J.Y. *Makromolekuare Chem. Rapid Commun.* **5**, 573 (1984).

[19] Varga, J., Garzó, G. *Acta Cimica Hungarica* **128**, 303 (1991).

[20] Morrow, D.R., Newman, B.A. *J. Appli. Polym. Sci.* **39**, 4944 (1968).

[21] De Rosa, C., Auriemma, F., Resconi, L. *Macromolecules* **38**, 10080 (2009).

[22] Auriemma, F., De Rosa, C., Boscato, T., Corradini, P. *Macromolecules* **34**, 4815 (2001).

[23] De Rosa, C., Auriemma, F., Supera, C., Talarico, G., Trallo, O. *Macromolecules* **37**, 1441 (2004).

[24] Lots, B., Graff, S., Wittmann, J.C. *J. Polym. Sci. Polym. Phys.* **24**, 2017 (1986).

[25] Sun, D. Zhang, R., Liu, Z. Huang, Y. Wang, Y. He, J. Han, B. Yang, G. *Macromolecules* **38**, 5617 (2005).

[26] Bahloul, W. Legare, V. B. David, L. Cassagnau, *P. J Polym Sci B Polym Phys.* **48**, 1213 (2010).

[27] Shimazaki, Y., Hojo, F., Takezawa, Y. *ACS Appl. Mater. Interfaces.* **1**, 225 (2009).

[28] Shimazaki, Y., Hojo, F., Takezawa, Y. *Appl. Phys. Lett.* **92**, 133309 (2008).

[29] Droval, G., Feller, J. F., Salagnac, P., Glouannec, P. *Polym. Adv. Technol.* **17**, 732 (2006).

[30] Bujard, P., Kuhnlein, G., Ino, S., Shiobara, T. IEEE Trans. *Compon., Packag., Manuf. Technol., Part A* **17**, 527 (1994).

[31] Lee, W. S., Yu, J. *Diamond Relat. Mater.* **14**, 1647 (2005).

[32] Gonon, P., Sylvestre, A., Teysseyre, J., Prior, C. *J. Mater. Sci.: Mater. Electron.* **12**, 81 (2001).

[33] Hussain, M., Oku, Y., Nakahira, A., Niihara, *K. Mater. Lett.* **26**, 177 (1996)

[34] Zhou, W., Wang, C., Ai, T., Wu, K., Zhao, F., Gu, H. *Composites, Part A* **40**, 830 (2009).

[35] He, H., Fu, R., Shen, Y., Han, Y., Song, X. Compos. Sci. Technol. **67**, 2493 (2007).

[37] Riley, F. L. *J. Am. Ceram. Soc.* **83**, 245 (2000).

[38] Wang, J., Yi, X. S. *J. Appl. Polym. Sci.* **89**, 3913 (2003).

[39] Yu, S., Hing, P., Hu, X. *Composites, Part A* **33**, 289 (2002).

[40] Kume, S., Yamada, I., Watari, K., Harada, I., Mitsuishi, K. J. *Am. Ceram. Soc.* **92**, 153 (2009).

[41] Lee, E. S., Lee, S. M., Shanefield, D. J., Cannon, W. R. *J. Am. Ceram. Soc.* **91**, 1169 (2008).

[42] Xie, S. H., Zhu, B. K., Li, J. B., Wei, X. Z., Xu, Z. K. *Polym. Test.* **23**, 797 (2004).

[43] Bae, J. W., Kim, W., Cho, S. H., Lee, S. H. *J. Mater. Sci.* **35**, 5907 (2000).

[44] Yung, K. C., Liem, H. J. Appl. Polym. Sci. **106**, 3587 (2007).

[45] Huang, M. T., Ishida, H. *J. Polym. Sci., Part B: Polym. Phys.* **37**, 2360 (1999).

[46] Koh, W. H. Electron. *Components Technol. Conf.* 343 (1996)

[47] Harrison, C., Weaver, S., Bertelsen, C.; Burgett, E., Hertel, N., Grulke, E. *J. Appl. Polym. Sci.* **109**, 2529 (2008).

[48] Ishida, H., Rimdusit, S. *Thermochim. Acta.* **32**, 177(1998).

[49] Hill, R. F., Supancic, P. H. *J. Am. Ceram. Soc.* **85**, 851 (2002).

[50] Chiang, T. H., Hsieh, T. E. *J. Inorg. Organomet. Polym.* **16**, 175 (2006).

[51] Zhou, W. Y., Qi, S. H., An, Q. L., Zhao, H. Z., Liu, N. L. *Mater. Res. Bull.* **42**, 1863 (2007).

[52] Lee, G. W., Park, M., Kim, J., Lee, J. I., Yoon, H. G. *Composites, Part A* **37**, 727 (2006).

[53] Xu, Y., Chung, D. D. L., Mroz, C. *Composites, Part A* **32**, 1749 (2001).

[54] Zeng, J., Fu, R., Shen, Y., He, H., Song, X. *Appl. Polym. Sci.* **113**, 2117 (2009).

# Chapter 2

# Formation of Highly Dispersed Ceramics Containing Polypropylene Nanocomposites by In-Situ Sol-Gel Reaction

## *2.1. Introduction*

Recently, polymer nanocomposite materials have attracted intense interest. Nanocomposite have various performance compared to the original polymer such as improved physical property [1]. The most important parameters that control the properties of these materials are related to the morphology and dispersion of inorganic filler. Nanolevel dispersion of inorganic filler is essential to achieve the above mentioned improvements.

Polypropylene (PP) is one of the most widely used polyolefin due to good mechanical propertis, high processability, low environmental load and high chemical resistance. PP-based nanocomposites have attracted particularly large expectation owing to its high demand in the market. However, it is difficult to achieve good dispersion of polar fillers in the nonpolar PP matrix. Method for overcoming this problem is addition of compatibilizer such as maleic anhydride grafted PP [2], organic modification filler surface [3], and using in-situ sol gel method [4,5]. The sol–gel process consists of hydrolysis and condensation reactions of metal alkoxides within a polymer matrix. These reactions lead to the formation of an inorganic network that is dispersed throughout the polymer matrix. Sun.et.al reported the preparation of PP/Silica nanocomposites using supercritical $CO_2$[5]. In their study, describe the preparation of

PP/silica nanocomposites using a two-step route. Tetraethoxysilane was first impregnated into PP films with the aid of supercritical $CO_2$, and then the nanocomposite was prepared by hydrolysis/condensation reaction of the films in acidic water. Possible limitations of the method are the necessity of thin films and the inapplicability to large-scale production based on a conventional melt-mixing technology.

In this research is to develop a more versatile strategy for the large-scale fabrication of nanosized metal oxide networks in the PP matrix. We use impregnation method for the pretreatment. It considered that precursor dissolved in a solvent impregnate for polymer and can prepare PP/common ceramics nanocomposites.

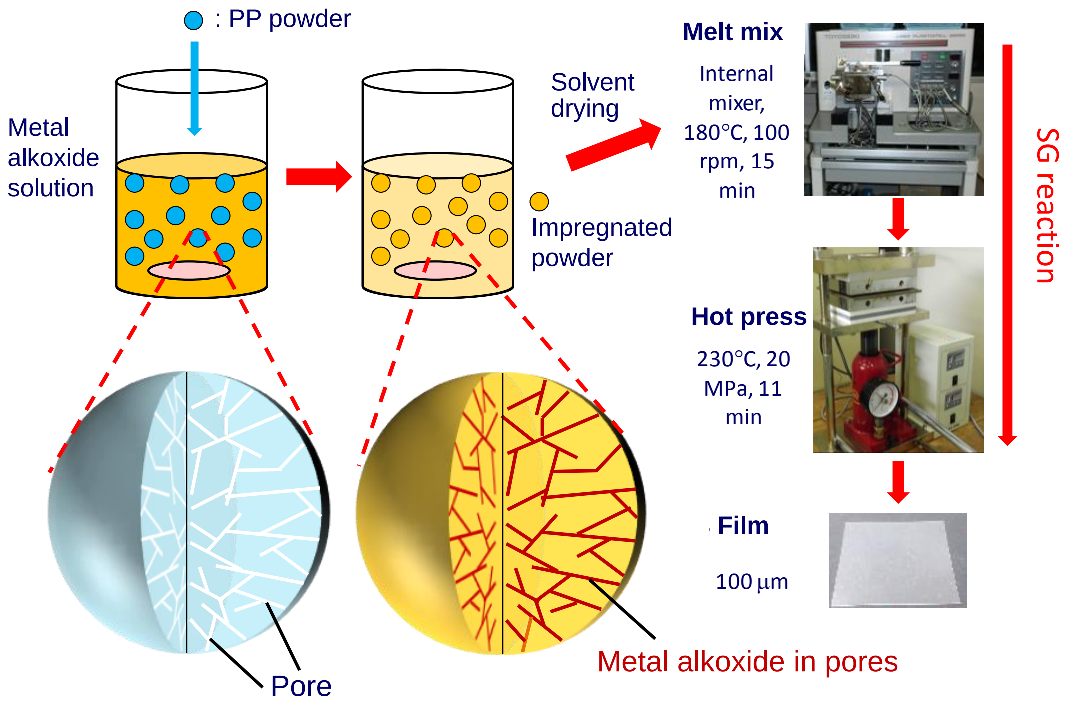

## *2.2. Experimental Section*

### *2.2.1. Materials*

PP powder was synthesized by slurry polymerization of propylene with a $MgCl_2$-supported Ziegler-Natta catalyst. Its *mmmm*, weight average molecular weight ($M_w$), and molecular weight distribution ($M_w/M_n$) are 98 mol%, 2.6 x $10^5$ and 5.69, respectively. Aluminum *i*-propoxide ($Al(OiPr)_3$), Titanium *i*-propoxide ($Ti(OiPr)_4$) was purchased from Sigma-Aldrich Co.. AO-50 as a stabilizer and LA-77 as a catalyst for the sol-gel reaction were donated by ADEKA Co., Ltd..

### *2.2.2. Sample preparation*

$Al(OiPr)_3$ or $Ti(OiPr)_4$ (corresponding to 3.0 wt% of metal oxide), AO-50, and LA-77 were dissolved in heptane. PP powder was soaked in the solution. $Al(OiPr)_3$ or $Ti(OiPr)_4$ was impregnated in PP for 3 - 9 h at 50 - 90ºC under $N_2$ (Scheme 2.1). After evaporating heptane, the mixture was pressed at 230°C under 20 MPa, then quenched at 100°C to obtain films with the thickness of 100 μm (Scheme 2.2). The sol-gel reaction proceeded to during the hot press.

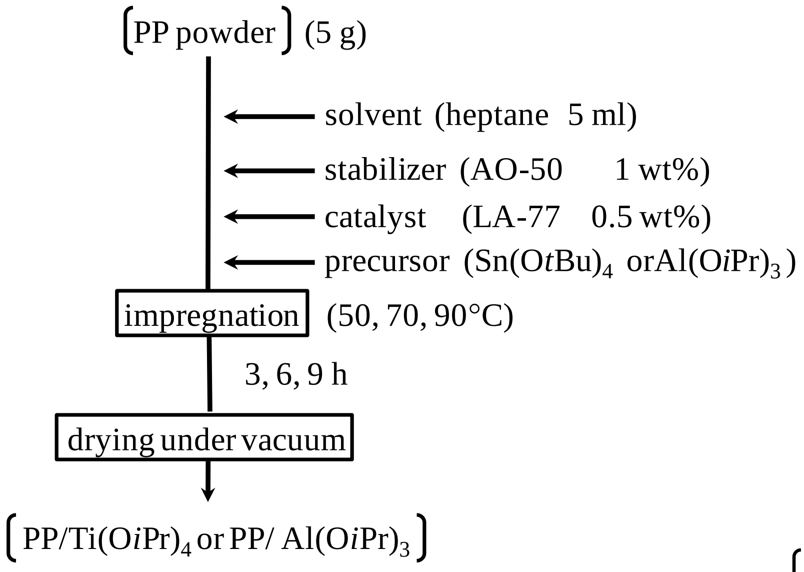

Scheme 2.1. Impregnation of PP powder and ceramics precursor

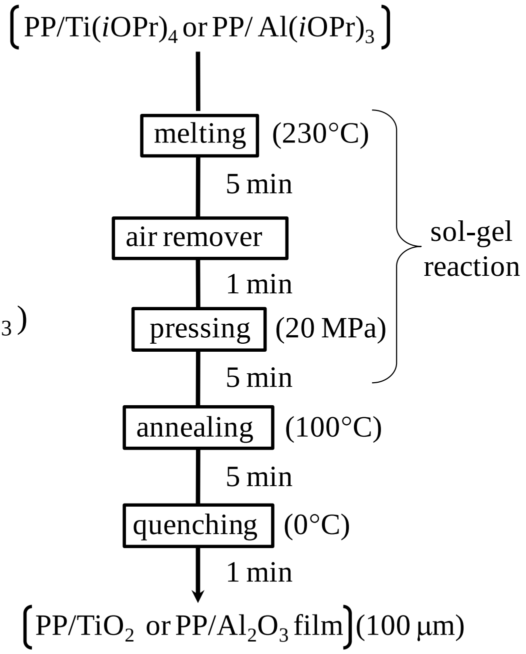

Scheme 2.2. Preparation of PP/$TiO_2$ or PP/$Al_2O_3$ film

### *2.2.3. Instrumentation*

Thermogravimetric analysis (TGA, TG-50, Metler Toledo) was used to determine the content of formed alumina in PP. Samples were heated up to 600°C at 20°C/min to burn out PP. The weight of the residue was regarded as that of alumina. The formation of alumina was confirmed by Fourier transform infrared spectroscopy (FTIR, 6100, JASCO). The dispersion of synthesized alumina in PP was observed by transmission electron microscope (TEM, H-7650, Hitachi) at an acceleration voltage of 100 kV. Sample films with the thickness of 100 nm were prepared using an ultramicrotome

(Reichent Ultracut FCS, Reica) equipped with a diamond knife.

### *2.3. Results and discussion*

Results of alumina contents obtained from TGA are shown in Table 2.1. The content was not affected by the conditions of the impregnation. The actual content was lower than the theoretical content (*ca*. 3 wt%), because of the volatilization of Al(O*i*Pr)$_3$ during the removal step of heptane or during the hot press.

Table 2.1. Filler contents in nanocomposites

| Sample | Impregnation temperature (°C) | Impregnation time (h) | Theoretical amount (wt%) | $TiO_2$ content (wt%) |
|---|---|---|---|---|
| PP/$TiO_2$ | 50 | 6 | 3 | 1.9 |
| | 70 | 6 | 3 | 1.8 |
| | 90 | 6 | 3 | 1.7 |
| | 50 | 3 | 3 | 1.7 |
| | 50 | 9 | 3 | 1.9 |
| PP/$Al_2O_3$ | 50 | 6 | 3 | 1.8 |
| | 70 | 6 | 3 | 1.9 |
| | 90 | 6 | 3 | 1.7 |
| | 50 | 3 | 3 | 1.8 |
| | 50 | 9 | 3 | 2.0 |

The synthesis of alumina in PP was confirmed by FTIR (Figure 2.1). After the sol-gel reaction, new two peaks appear at around 590 and 700 cm$^{-1}$, both of which were assigned to the stretching vibration of Al-O-Al. These peaks indicated the formation of alumina in PP.

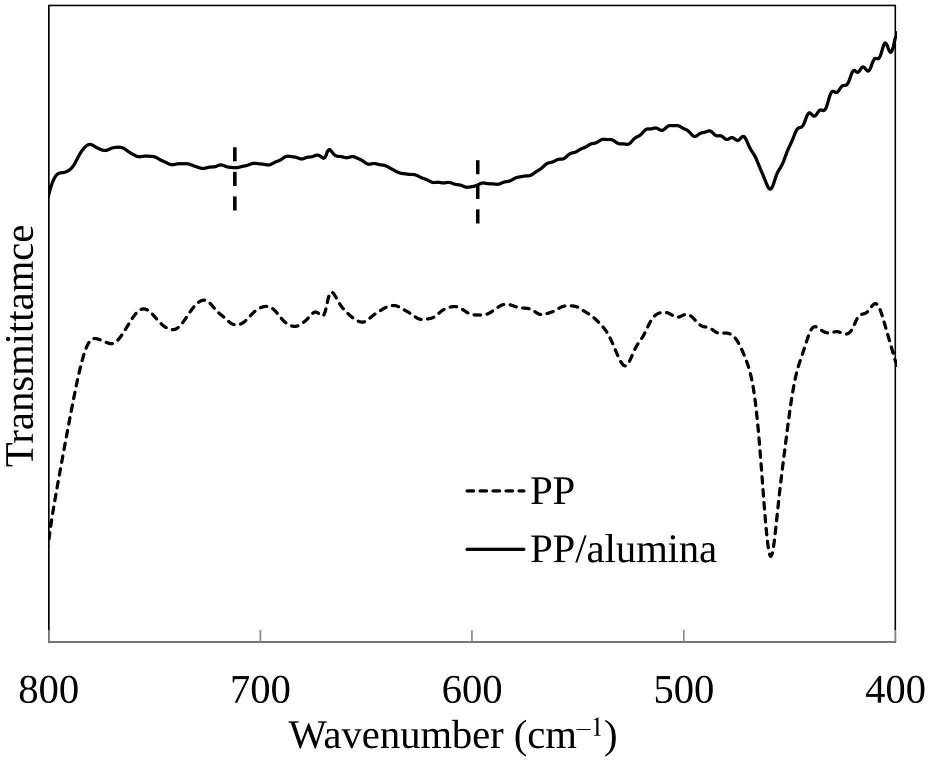

Figure 2.1. IR spectra of PP and PP/$Al_2O_3$ films

Influences of the impregnation temperature and time on the dispersion of alumina in PP/$Al_2O_3$ were investigated by TEM (Figures 2.2 and 2.3). As shown in Figure 2.2, the dispersion was not significantly affected by the impregnation temperature.

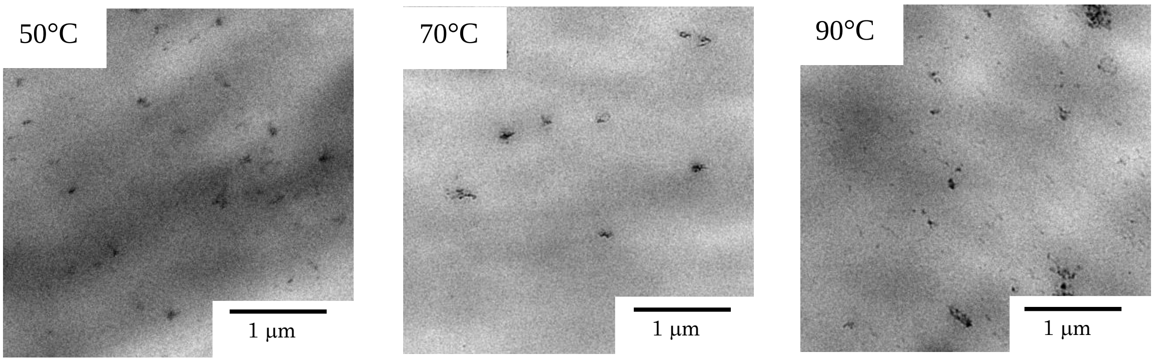

Figure 2.2. TEM images of PP/$Al_2O_3$ prepared at the different impregnation temperatures

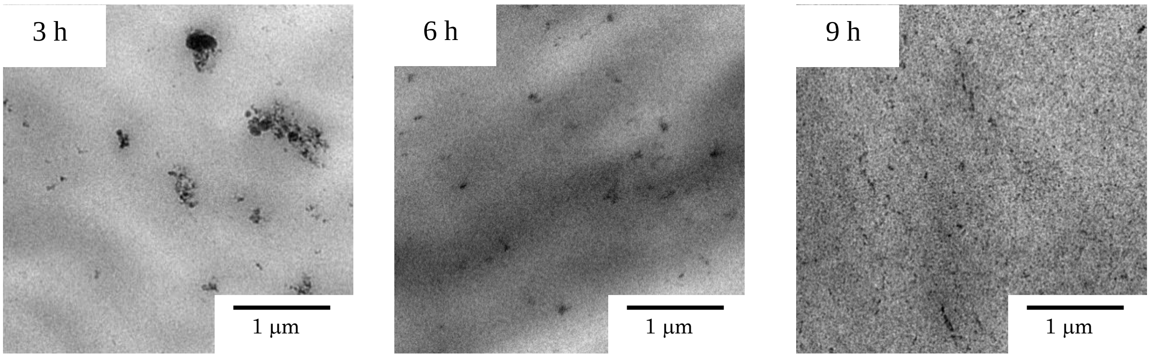

Figure 2.3. TEM images of PP/$Al_2O_3$ prepared at different impregnation times

Figure 2.3 shows alumina particles were highly dispersed in PP by prolonging the impregnate time though a shorter impregnation time led to the formation of alumina aggregates in PP. It was considered the longer the impregnation time was, the more the precursor penetrated uniformly into pores of PP powder, resulting in the improvement of the alumina dispersion in PP.

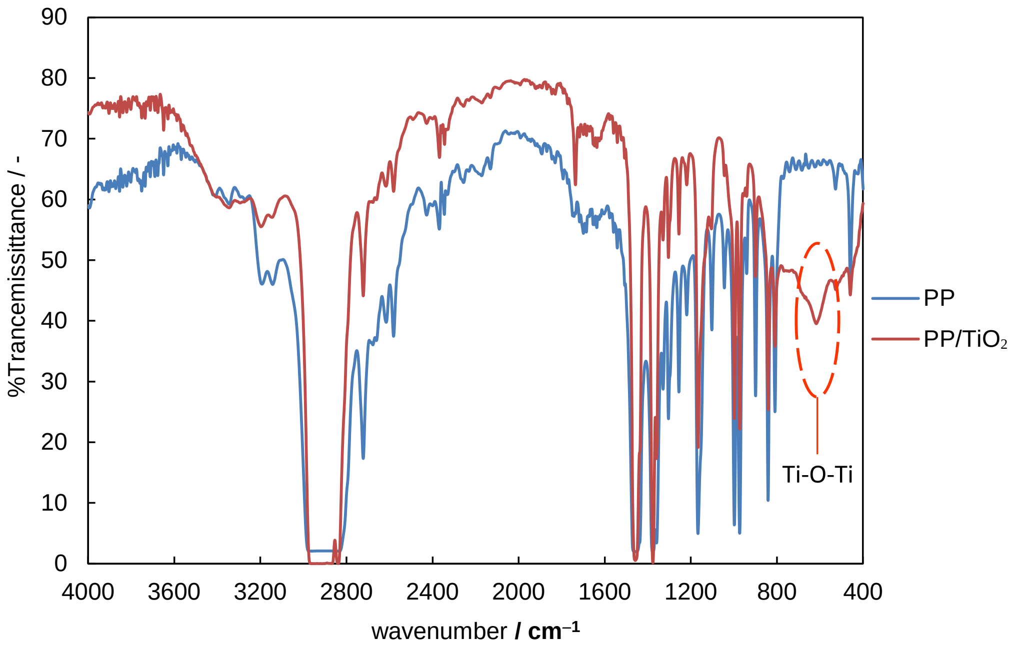

The synthesis of titania in PP was confirmed by FTIR (Figure 2.3). After the sol-gel reaction, new two peaks appear at around 600 cm$^{-1}$ of which were assigned to the stretching vibration of Ti-O-Ti. These peaks indicated the formation of titania in PP. On the other hand, the Ti–O–C absorption around 1070 cm$^{-1}$ cannot seen in the spectrum, suggesting a positive influence of the impregnation for promoting the sol–gel reaction in the melt mixing.

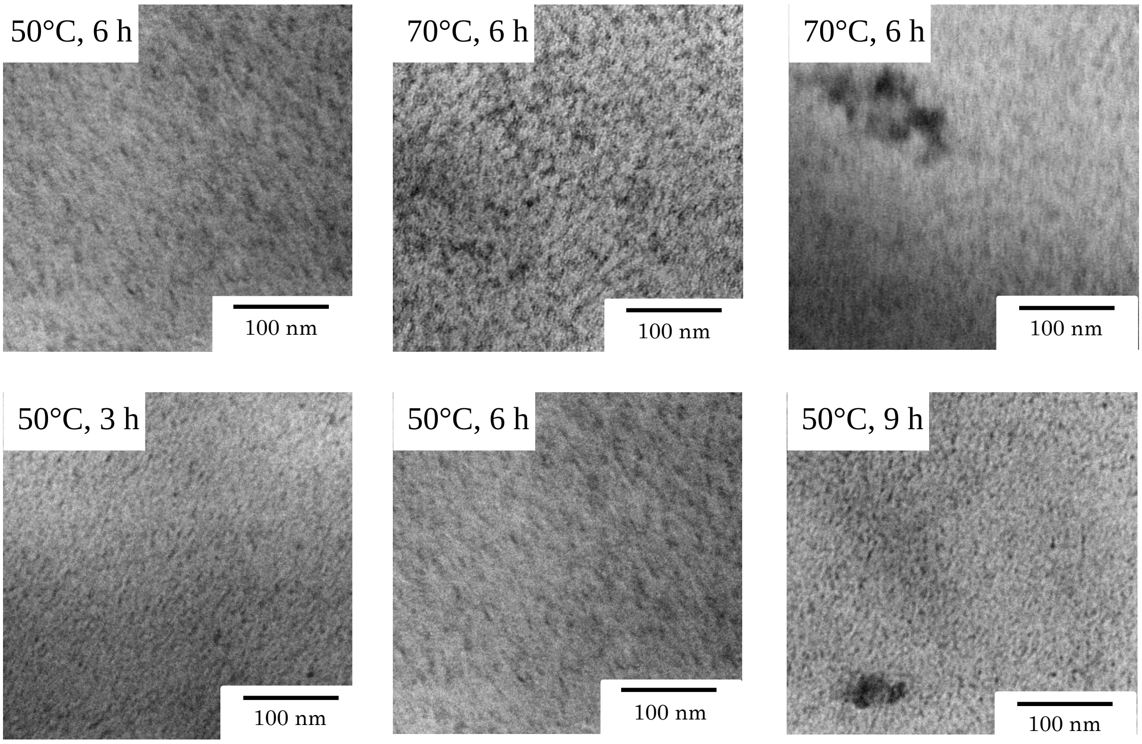

Figure 2.5. TEM images of PP/$TiO_2$ nanocomposites (influence of impregnation temp. and time)

In Figure 2.5, the Filler dispersion was not affected by the impregnation temperature.

The $TiO_2$ particles were highly dispersed in PP by longer impregnation time. It led to long impregnation time led to highly dispersed filler.

Figure 2.6 shows the UV- Vis spectra of PP and PP/$TiO_2$ (impregnation condition: 50°C, 9 h) nanocomposites films (30 μm), recorded in the transmittance mode. The UV shielding property, the sol-gel based PP/$TiO_2$ nanocomposites films are highly transparent (over 80%) in the visible region, comparable to PP film, as shown in UV-Vis spectra.

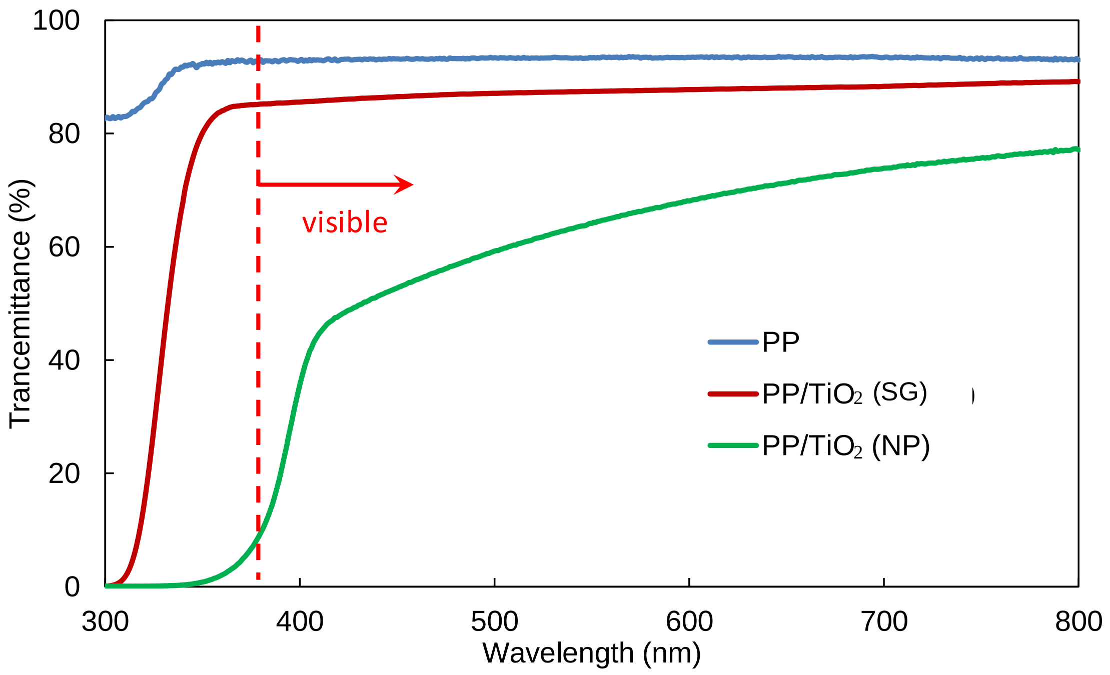

Figure 2.6 UV-vis spectra of based PP/$TiO_2$ nanocomposites

The PP/$TiO_2$ nanocomposites obtained via direct melt mixing of $TiO_2$ nano particles films absorb UV light starting attribute to the $TiO_2$ absorption spectra of around 380 nm. The sol-gel based PP/$TiO_2$ nanocomposites films absorb UV light, starting at around 350 nm (λonset) and blocked completely the transmittance of UV- light in the region 200-295 nm. The “blue shift” of the absorption edge among the nanohybrids is attributed to the differences in band gap which was considered to be affected by quantum effect for nanosized $TiO_2$ particles. The blue shift can be used to find the approximate organized domain size from the relationship derived by Brus from a particle in a sphere model for relating band gap shift to particle radius [6]. Even though our $TiO_2$ nanoparticles formed in PP were amorphous due to the lack of a crystallization process, the observed dramatic blue shifts in the absorption onset could not be accounted unless the particle sizes were around 5-10 nm.

### *2.4. References*

[1] Okada, A., Usuki, A., *Macromol. Mater. Eng*. **291**, 1449 (2006).

[2] Asuka, K., Liu, B., Terano, M., Nitta, K. *Macromol. Rapid Commun.* **27**, 910 (2006).

[3] Hasegawa, N., Kawasumi, M., Kato, M., Usuki, A., Okada, A., *J. Appl. Polym. Sci.* **67**, 87 (1998).

[4] Christèle, B., Emmanuel, B., Elodie, B. L., Philippe, C., Laurent, D., Nathalie, Z. *Polymer* **46**, 9965 (2005).

[5] Sun, D., Zhang, R., Liu, Z., Huang, Y., Wang, Y., He, J., Han, B., Yang, G. *Macromolecules* **38**, 5617 (2005).

[6] Reddy, K. M., Manorama, S. V., Reddy, A. R. *Mater Chem Phys.* **78**, 239 (2002)

# Chapter 3

# Analysis of Filler Network Structure in Polypropylene Nanocomposite Prepared by Impregnation Method

## *3.1. Introduction*

Polypropylene (PP) is an important versatile plastic due to good mechanical properties, low environmental load and high chemical resistance. In order to expand its applications, tremendous efforts have been devoted to develop PP nanocomposites, where a new functionality originated from the nature of fillers is incorporated without scarifying processability of conventional PP[1,2]. Especially, highly thermal conductivity of PP is one of a target that has long been interested in high temperature applications such as the heat sinks in automobile. Thermal conductivity of polymer based-nanocomposites has been known to be greatly affected by the formation of a network[3]. However, poor compatibility of PP matrix and the organic fillers having polar nature results in a serious aggregation, thus preventing the network formation. Accordingly, the improvement of mechanical properties and functionalities are not obtained. The most frequently used method to overcome this problem is the addition of a compatibilizer. However, the inclusion of compatibility often leads to soft and non-bonded interfaces on nanofillers that limit the reinforcement.

The sol-gel reaction is one of the versatile methods to design network structures. Recently, we have reported a new approach for preparing PP nanocomposites without the use compatibilizer by the aid of impregnation and sol-gel techniques. Porosity of PP powder generated during catalyzed polymerization is impregnated with metal alkoxide before converting into metal oxide in the subsequent treatments and melt mixing. Nanoparticles formed in the confined porosity are extremely well-dispersed, leading to the formation of an inorganic network throughout the polymer matrix.

In this work, the *in-situ* formation of $Al_2O_3$ nanoparticle in polymer matrix by sol-gel method was applied to prepare PP/$Al_2O_3$ nanocomposites. The effect of $Al_2O_3$ loadings on the dispersion of nanoparticles and the thermal conductivity of nanocomposites were investigated.

## 3.2. Experiments

### 3.2.1. Materials

PP reactor powder was prepared from polymerization of propylene using a Ziegler-Natta catalyst ($M_w = 2.6 \times 10^5$, *mmmm* = 98 mol%, $M_w/M_n = 5.69$). Aluminum *i*-propoxide ($Al(O\textit{i}Pr)_3$) was purchased from Sigma-Aldrich Co. AO-50 and LA-77 as polymer stabilizer and condensation catalyst were donated from ADEKA Co., Ltd. $Al_2O_3$ nanoparticles (NP) having diameter of 15 nm were purchased from Nippon Aerosil Co., Ltd. Toluene, Heptane, Hexane, xyline, *i*-Propanol, and t-Buranol as solvent were purchased from Kanto Chemical Co., Ltd.

### *3.2.2. Sample preparation*

PP/$Al_2O_3$ nanocomposites denoted as PP/$Al_2O_3$ (SG) were prepared by *in-situ* formation of $Al_2O_3$ network in polymer during melt mixing (Scheme 3.1). Al(O*i*Pr)$_3$ precursor (equivalent to the $Al_2O_3$ content of 1.0-20 wt%) was impregnated into PP powder using heptane as solvent. The suspension was stirred at 50°C for 12 h in the presence of AO-50 stabilizer and LA-77 catalyst to obtain PP/Al(*i*OPr)$_3$ polymer precursor. After drying the resultant polymer under vacuo (*t*-Butanol was using freeze-drying), the powder was subjected to melt mix, where the sol-gel (SG) reaction of the precursor in PP powder proceeded. 5.0-20 wt% of PP/$Al_2O_3$ (SG+NP) nanocomposites were prepared by melt mixing PP/$Al_2O_3$ (SG) having $Al_2O_3$ content of 2.7 wt% with a desired amount of pre-formed $Al_2O_3$ nanoparticles. The reference samples of PP/$Al_2O_3$ nanocomposites were also prepared by melt mixing pristine PP powder with $Al_2O_3$ nanoparticles. The sample films of 100 μm for all nanocomposites samples were prepared for the subsequent analysis.

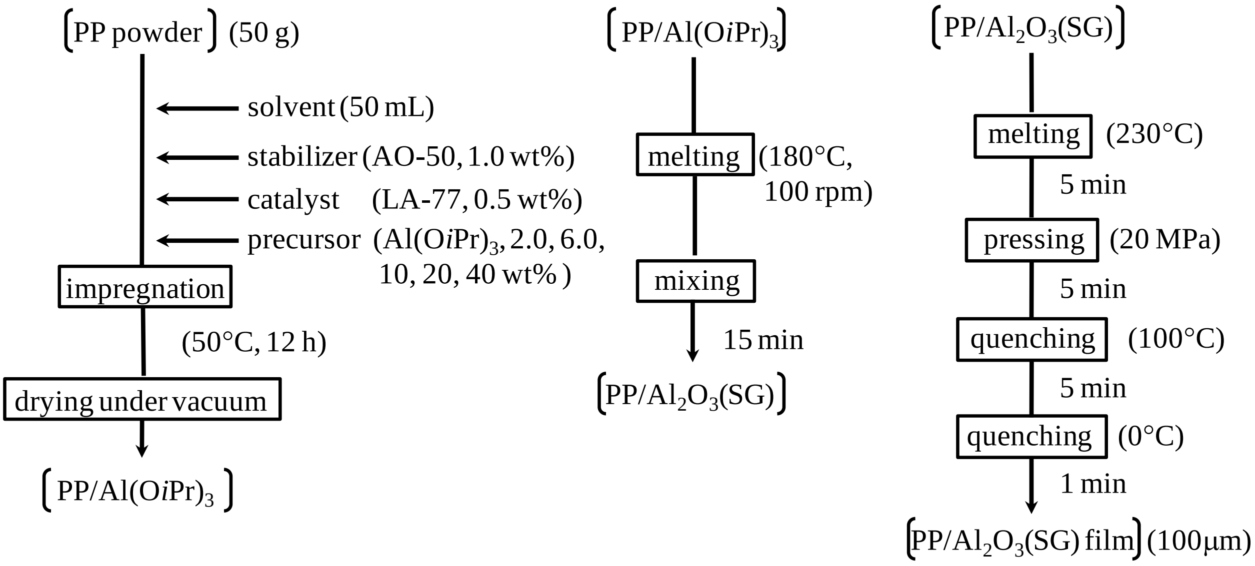

Scheme 3.1. The preparation of PP/ $Al_2O_3$ nanocomposites by sol-gel method

### 3.2.3. Characterization

$Al_2O_3$ content was analyzed by determining the weight of product residue after burning off PP matrix using thermogravimetry analysis (TGA, TG-50 Metler Toledo). The samples were heated from room temperature to 600°C at the heating rate of 20°C/min. Dispersion state of nanoparticles was evaluated by transmission electron microscope (TEM, H-7650, Hitachi). TEM samples of ultrathin section (thickness of 100 nm) were prepared using an ultramicrotome (Reichent Ultracut FCS, Reica). The network formation in PP nanocomposites was characterized by frequency dependence of melt viscoelastic measurement. The measurements were performed at 180°C with a frequency range from 100 to 0.01 rad/s under $N_2$ atmosphere. The thermal conductivity of PP and PP/$Al_2O_3$ nanocomposites was measured by hot-disc method (ISO22007-2).

## *3.3. Results and discussion*

### *3.3.1. Preparation of highly thermal conductive nanocomposite*

Table 3.1　$Al_2O_3$ content in PP/$Al_2O_3$(SG)

Table 1.　$Al_2O_3$ content in PP/$Al_2O_3$(SG)

| Sample | Estimated amount (wt%) | $Al_2O_3$ content (wt%) |
|---|---|---|
| PP/$Al_2O_3$(SG) | 1.0 | 0.9 |
| | 3.0 | 2.7 |
| | 5.0 | 4.8 |
| | 10.0 | 8.7 |
| | 20.0 | 15.3 |

Table 3.1 shows the $Al_2O_3$ content in PP/$Al_2O_3$(SG) nanocomposites after melt mixing. The $Al_2O_3$ content was found to be slightly lower than the theoretical value for all samples. This was believed to originate from the volatilization of $Al(OiPr)_3$ precursor during melt mixing.

The dispersion state of $Al_2O_3$ nanoparticles prepared by *in-situ* sol-gel method was observed by TEM (Figure 3.1).　Formed $Al_2O_3$ nanoparticles were highly dispersed in PP matrix up to 2.7 wt% content.　Further increase of the $Al_2O_3$ content to 4.8 wt% resulted in a significant agglomeration of nanoparticles.　It is considered that the confined porosity of PP as well as the high viscosity of PP in melt state prevented the agglomeration of nanoparticles.　However, the excessive addition of $Al(O_iPr)_3$ precursor resulted in the overflowing of precursor from the pores, which led to the agglomeration of formed nanoparticles. In order to avoid the overflowing of precursor at high filler loading, the PP/$Al_2O_3$ nanocomposites were prepared by melt mixing PP/$Al_2O_3$ (SG, 2.7 wt%) nanocpmposites with 3 wt% of pre-formed $Al_2O_3$ nanoparticles. We found that the hybrid composites exhibited better dispersion compared to 4.8 wt% of PP/$Al_2O_3$(SG) prepared by sol-gel method (Figure 3.1(d)).

(a) PP/$Al_2O_3$(SG) 0.9 wt% (b) PP/$Al_2O_3$(SG) 2.7 wt%

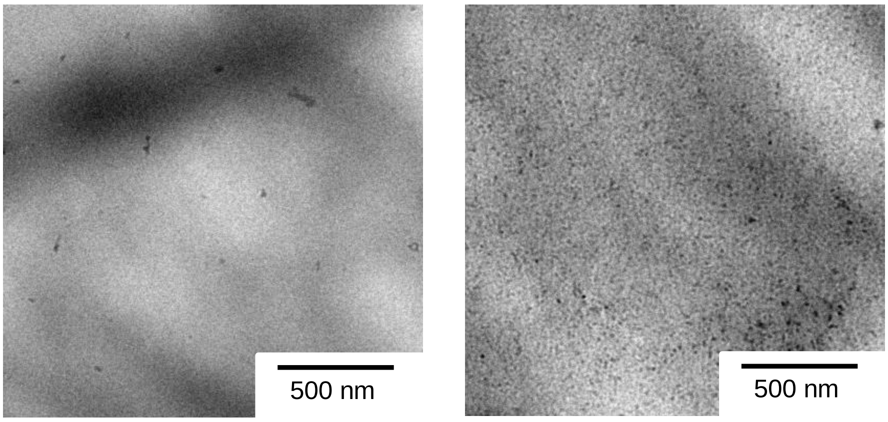

(c) PP/$Al_2O_3$(SG) 4.8 wt% (d) PP/$Al_2O_3$(SG+NP) 5.0 wt%

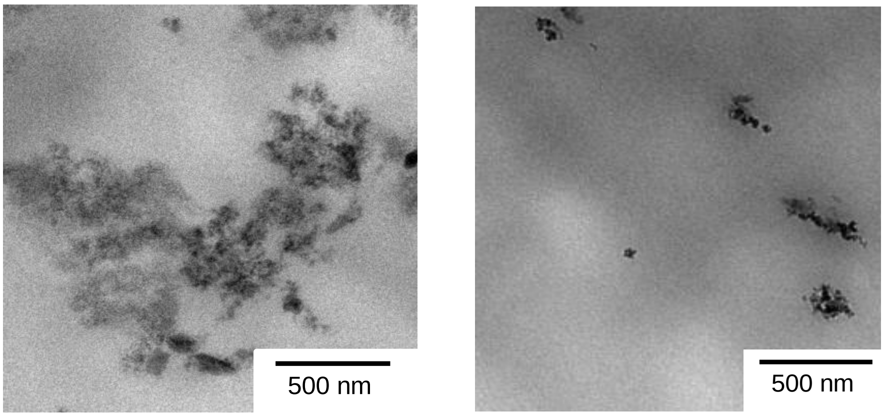

Figure 3.1. TEM images of PP/$Al_2O_3$ nanocomposites

The effect of $Al_2O_3$ contents on the network formation of PP/$Al_2O_3$(SG) and

$PP/Al_2O_3$(NP) nanocomposites was investigated by viscoelastic measurement (Figure 3.2, 3.3). When the $Al_2O_3$ content was higher than 2.7 wt%, a transition from liquid-like to solid-like viscoelastic behavior was observed at $PP/Al_2O_3$(SG). This nonterminal low frequency behavior can be attributed to a filler network formation. The storage modulus of $PP/Al_2O_3$(SG) with 4.8 wt% $Al_2O_3$ content was found to be lower than that of 2.7 wt% content. This was believed to be due to the large agglomeration of nanoparticles at high loading as observed by TEM. Although, as can be seen in Figure 3.3, the $PP/Al_2O_3$(NP) nanocomposites exhibited the disappearance or depression of the terminal flow even at 5 wt% of the $Al_2O_3$ contents. The sol gel technic can form network at low filler loading.

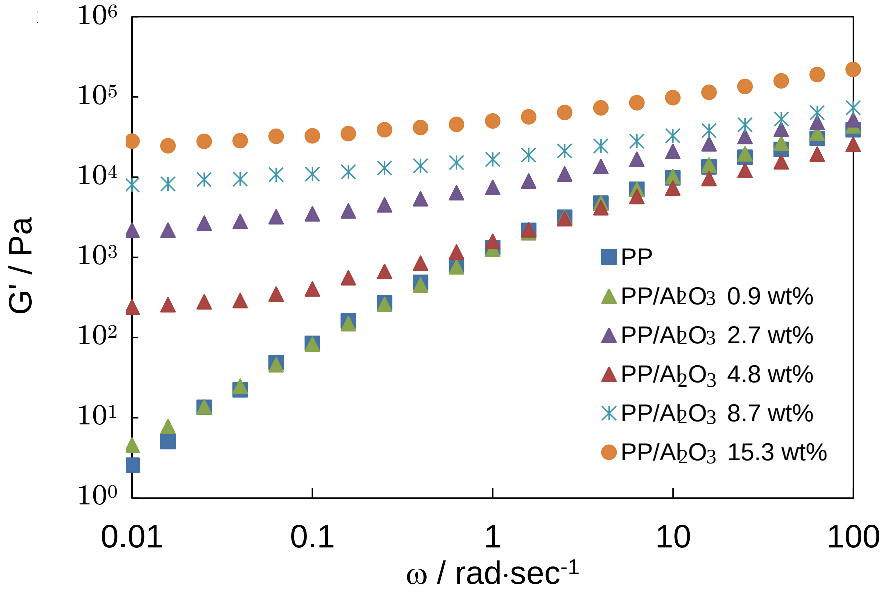

Figure 3.2 Viscoelastic properties of PP and $PP/Al_2O_3$(SG)

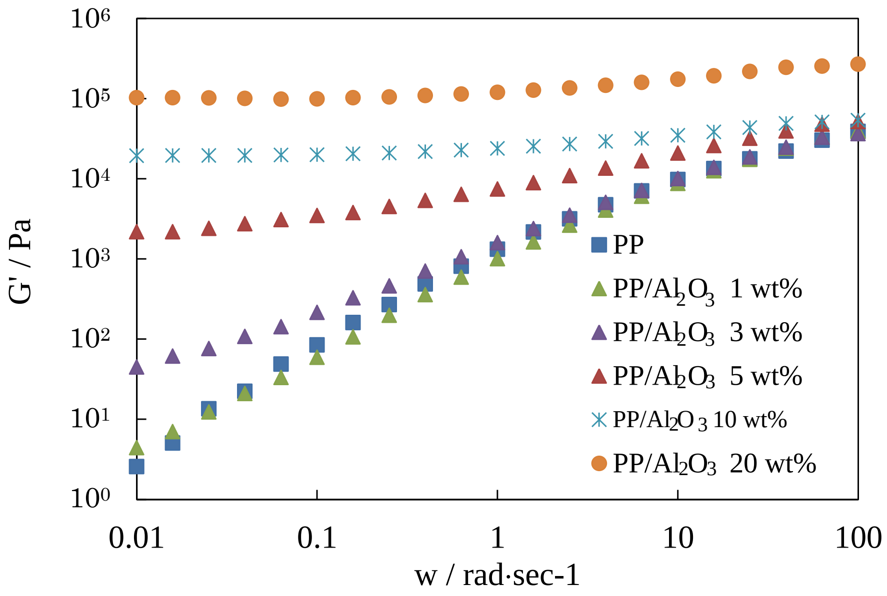

Figure 3.3.　Viscoelastic properties of PP and PP/$Al_2O_3$(NP)

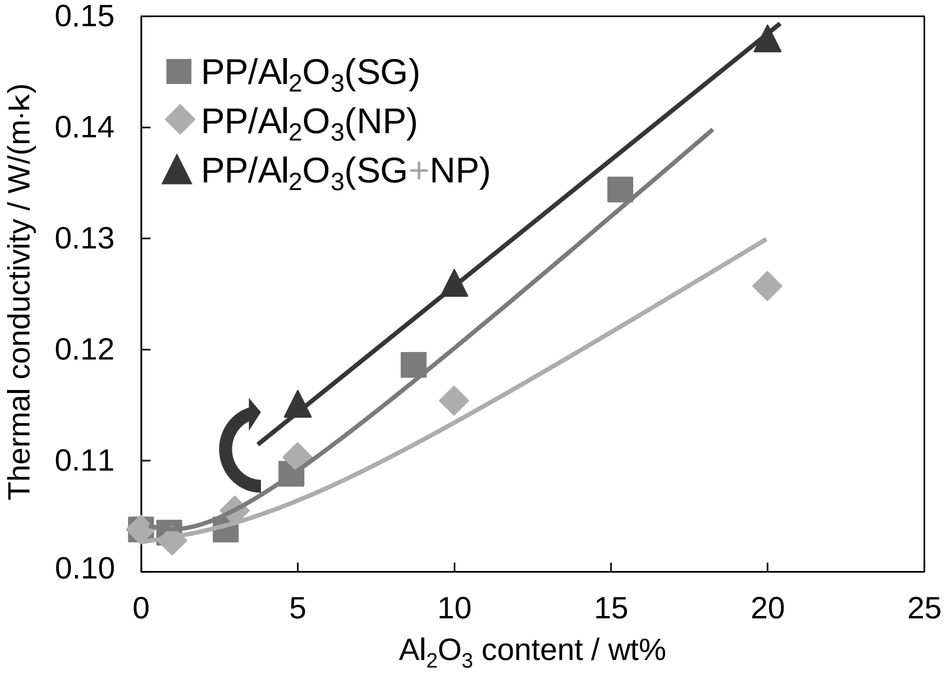

Figure 3.4.　Thermal conductivity of PP/$Al_2O_3$ samples

The thermal conductivity of PP and PP/$Al_2O_3$ nanocomposites were measured by hot-disc method (Figure 3.4). At low filler loading, all PP/$Al_2O_3$ nanocomposites had similar level of thermal conductivity. The increase of filler content increased thermal conductivity, in which the higher thermal conductivity was found for PP/$Al_2O_3$(SG) nanocomposites prepared by sol-gel method as compared to the conventional melt mixing at the same filler loadings. This was attributed to the enchantment of nanoparticle dispersion with the aid of sol-gel method. Further enhancement of conductivity was observed when the nanocomposites were prepared by sol-gel method in combination with pre-formed nanoparticles due to the improvement of dispersion at high loadings.

The dispersion state of $Al_2O_3$ nanoparticles prepared by *in-situ* sol-gel method using several solutions were observed by TEM (Figure 3.5).

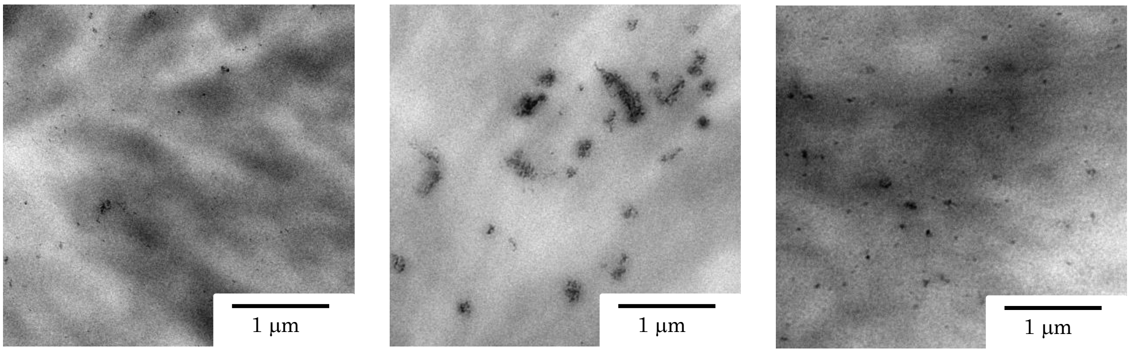

(a) Heptane (b) *i*-Propanol (c) *t*-Butanol (freeze drying)

Figure 3.5 TEM images of PP/$Al_2O_3$ (3 wt%) using several solution

The dispersion state of PP/$Al_2O_3$ using non-polar solution of heptane was nanosize and well dispersion compared with polar solvent of *i*-propanol. Large aggregates were formed by *i*-propanol. However, filler diameter and dispersion PP/$Al_2O_3$ polar solvent of *t*-Butanol was well dispersed. It suggest that, precursor was leaking from pores in PP powder under drying of solvent by using a polar solvent. Though, it was possible to prevent the elution of precursor by freeze-drying which led to high dispersion of the filler.

PP/$Al_2O_3$ nanocomposites was investigated by viscoelastic measurement (Figure 3.6).

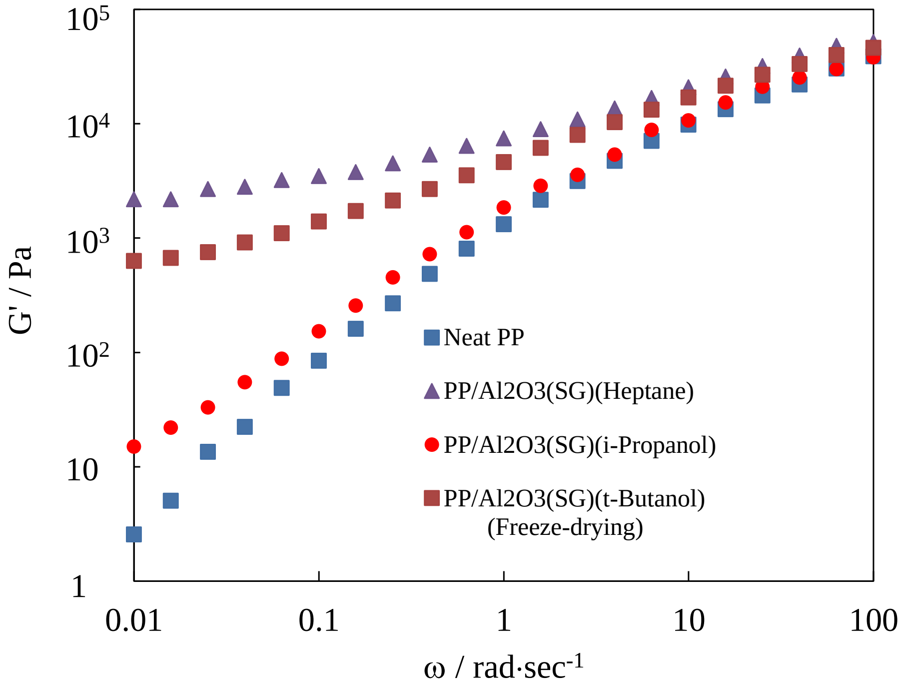

Figure 3.6 Viscoelastic properties of PP and PP/$Al_2O_3$(SG)(3 wt%)

As can be seen in Figure 3.6 PP/$Al_2O_3$(SG)(*i*-propanol) nanocomposites did not exhibit the disappearance of the terminal flow. It estimated that, the formation of large agglomeration of nanoparticles as observed by TEM. However, terminal flow of PP/$Al_2O_3$(SG)( *t*-Butanol) change from liquid-like to solid-like viscoelastic behavior was observed, which can be attributed to a filler network formation.

The thermal conductivity of PP/$Al_2O_3$(NP) and PP/$Al_2O_3$(SG+NP) nanocomposites were measured by hot-disc method (Figure 3.7).

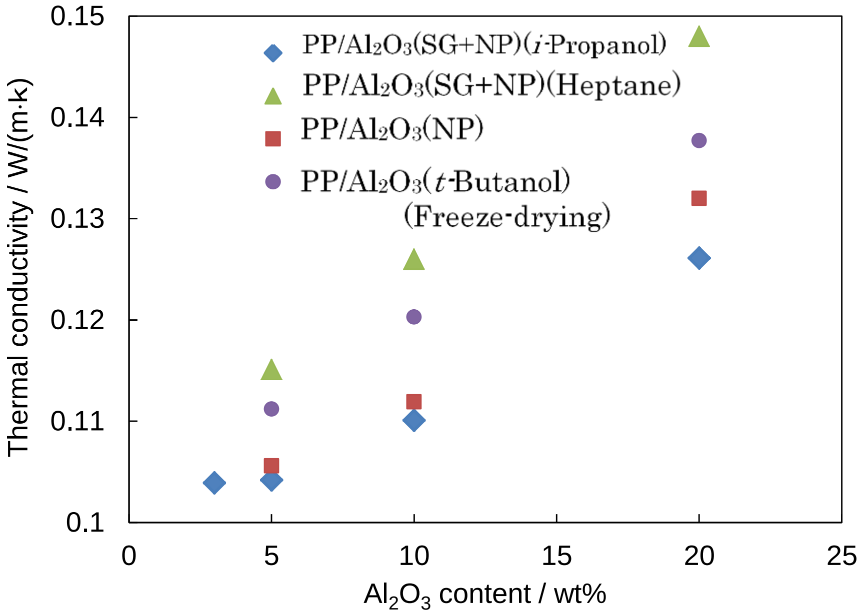

Figure 3.7 Thermal conductivity of PP/$Al_2O_3$ samples

Thermal conductivity of PP/$Al_2O_3$(SG+NP)(*i*-propanol) was lower than PP/$Al_2O_3$(NP). However, PP/$Al_2O_3$(SG+NP)(*t*-butanol) was intermediate in thermal conductivity between PP/$Al_2O_3$(NP) and PP/$Al_2O_3$(SG+NP)(Heptane). Thus, path of the heat of PP/$Al_2O_3$(SG+NP)(*t*-butanol) was much more than PP/$Al_2O_3$(SG+NP)(*i*-propanol). This was believed to be due to the impregnation of precursor in pores of PP reactor powder.

The dispersion state of $Al_2O_3$ nanoparticles prepared by *in-situ* sol-gel method using several polar solutions were observed by TEM (Figure 3.8).

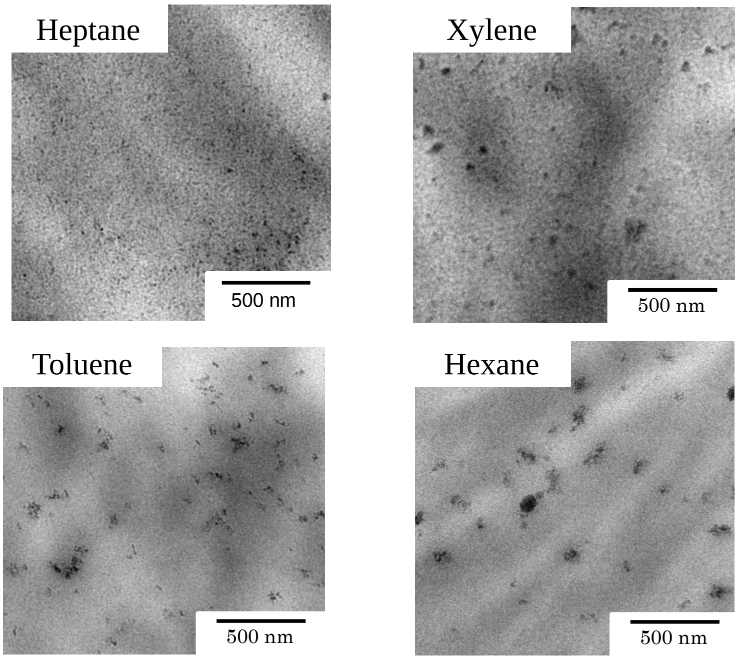

Figure 3.8 TEM images of PP/$Al_2O_3$ (3 wt%) using several polar solution

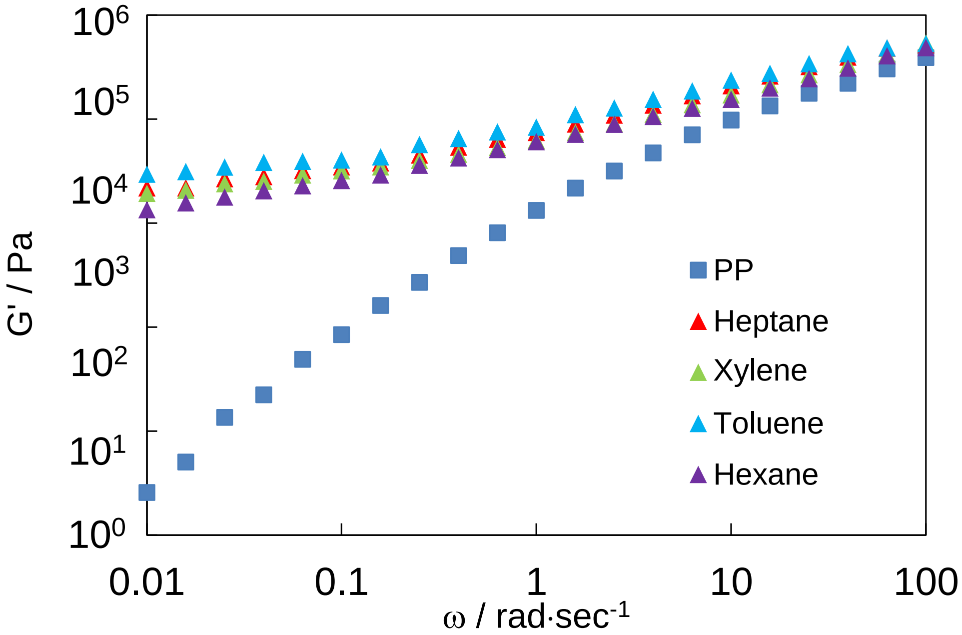

Figure 3.9 Viscoelastic properties of PP and PP/$Al_2O_3$(SG)(3 wt%) using several polar solvent

Synthesized $Al_2O_3$ particles basically had a nano-size and were homogeneously dispersed in PP matrix except for a minor fraction of larger nanoparticles. The frequency of these larger nanoparticles was relatively higher for Hexane. As shown in Figure 3.9, the order of the storage modulus at low frequency area was Xylene> Toluene>Heptane> Hexane.

Table 3.2 Hildebrand solubility parameter

| | $\delta$ ($cal^{1/2}\cdot cm^{-3/2}$) |
|---|---|
| PP | 9.3 |
| Xylene | 8.8 |
| Toluene | 8.8 |
| Heptan | 7.4 |
| Hexane | 7.3 |

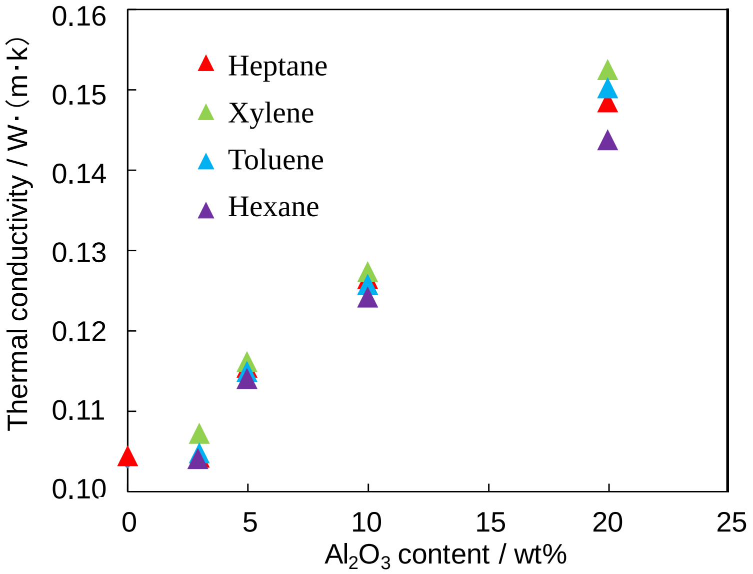

Figure 3.7 Thermal conductivity of PP/$Al_2O_3$(SG+NP) samples using several polar solvent

Hildebrand solubility parameter was shown in Table 3.2.

Thermal conductivity of PP/$Al_2O_3$(SG+NP) becomes higher foe solvent that has SP value closer to that of PP (Figure 3.7). It estimated that, the solvent which having a strong affinity for PP was provide the storage modulus and the thermal conductivity.

## *3.4. Conclusions*

In this report, a series of PP/$Al_2O_3$ nanocomposites were prepared by *in-situ* formation of $Al_2O_3$ nanoparticles via sol-gel method. The obtained nanocomposites exhibited excellent dispersion of nanoparticles up to 2.7 wt% content, while the agglomeration occurred at higher loading. The improvement of nanoparticle dispersion at high filler loadings was successfully achieved through the hybrid concept, where the pre-formed nanoparticles were combined. Highly dispersion of nanoparticles at high loading resulted in the improvement of thermal conductivity. This technique is an effective strategy to develop highly dispersed nanocomposites with high loadings without the use of compatibilizer.

## *3.5. References*

[1] Okada, A., Usuki , A. *Macromol. Mater. Eng.* **291**, 1449 (2006).

[2] Asuka, K., Liu, B., Terano, M., Nitta, K. *Macromol. Rapid Commun.* **27**, 910 (2006).

[3] Li, T.L., Hsu, S.L.C., *J. Phys. Chem. B.* **114**, 6825 (2010)

# Chapter 4

# General Conclusions

In this study, PP/metal oxide nanocomposites were prepared through the impregnation of PP amorphous part with metal alkoxide and subsequent sol-gel reaction. A new approach for preparing better PP nanocomposites is to apply the sol-gel technique. We tried to impregnation and sol-gel reaction of metal alkoxide in porosity of PP reactor powder, which have a large number of pores derived by the structure of the catalyst. It leads to the formation of an inorganic network throughout the polymer matrix. It was attempted to develop more versatile strategy for the large-scale fabrication of nanosized metal oxide network in the PP matrix. In chapter2, the metal oxide particle was prepared with the impregnation time of 9 h makes homogenously dispersed and formed small aggregates in the matrix. It was suggested that long time of impregnation method impregnate the precursor into pores of PP powder surface. It considered that long period of time reach the impregnation equilibrium.

In chapter 3, PP/$Al_2O_3$ nanocomposites was prepared using impregnation method, where a precursor dissolved in solvent was impregnated into pores of PP reactor powder prior to sol-gel reaction. Thermal conductivity may be achieved by introducing a network structure of $Al_2O_3$ within polymer matrix. The thermal conductivity was improved by the method, owing to the formation of $Al_2O_3$ filler network. Further, combination of impregnation and sol-gel methods with nanoparticle was found to be quite effective for achieving the high thermal conductivity of PP nanocomposites.

Finally, novel design of metal oxide network in polypropylene using sol-gel method using impregnation method achieved and the development is expected to expand both academic and industrial area.

## Achievements

### ＜Original Article＞

"Versatile Strategy for Fabrication of Polypropylene Nanocomposites with Inorganic Network Structures based on Catalyzed in-situ Sol-Gel Reaction during Melt Mixing"
Kei Kaneko, Nitin Yadav, Kengo Takeuchi, Bulbul Maira, Minoru Terano, Toshiaki Taniike, Composites Science and Technology, 2014, 102, 120-125.

### ＜International conference＞

1. “Formation of Highly Dispersed Alumina Containing Nanocomposites by In-Situ Sol-Gel Reaction”
9th International Symposium on Weatherability 3rd International Workshop on Polymer Degradation and Stability, Tokyo, Japan, Mar. 2013.

2. “Analysis of Filler Network Structure in Polypropylene Nanocomposite Prepared by Impregnation Method”
International Symposium for Green-Innovation Polymers, Kanazawa, Japan, Mar. 2014.

3. “Highly thermal conductive polypropylene nanocomposites having $Al_2O_3$ network formed by the combination of impregnation and sol-gel methods.”
5th International Conference on Polyolefin Characterization, Valencia, Spain, Sep. 2014.

4. “Highly Thermal Conductive Polypropylene Nanocomposites Having $Al_2O_3$ Network Formed Through Impregnation” 10th International Symposium on Weatherability, Gunma, Japan, Mar. 2015

＜Domestic conference＞

1. 新規含浸Sol-gel法を用いた機能性無機ネットワーク構造含有ポリプロピレン系ナノコンポジットの合成
マテリアルライフ学会第17回春季研究発表会、東京、2013年、3月

2. ポリプロピレンの非晶部を利用したナノフィラーの構造制御と溶融物性に与える影響
第63回高分子学会年次大会、京都、2013、5月

3. 含浸ゾルゲル法を利用した高熱伝導ポリプロピレン系アルミナナノコンポジットの調製
マテリアルライフ学会第24回研究発表会、東京、2013、7月

4. 含侵ゾルゲル法によりポリプロピレン中にin-situ合成したフィラーネットワーク構造の解析
第62回高分子学会討論会、金沢、2013年、9月

5. 含浸ゾルゲル法と粒子混練を組み合わせたポリプロピレン/アルミナナノコンポジットの高熱伝導化

平成25年度北陸地区講演会と研究発表会、石川、2013、11月

6. 含浸ゾルゲル法を用いたポリプロピレン系ナノコンポジットの調製と特性分析

第4回ポリオレフィン研究若手会、石川、2014、1月

7. 各種溶媒を用いた含浸ゾルゲル法による高熱伝導ポリプロピレン系アルミナナノコンポジットの合成

マテリアルライフ学会第18回春季研究発表会、東京、2014、3月

8. 紫外光遮光特性を有するポリプロピレン/酸化亜鉛ナノコンポジットの含浸ゾルゲル法による合成

マテリアルライフ学会第25回研究発表会、東京、2014、7月

9. 含浸ゾルゲル法によるポリプロピレン微粒子中でのアルミナネットワークの形成

マテリアルライフ学会第26回研究発表会、群馬、2015、7月

**Sub-theme report**

# Synthesis of the Poly Styrene-b-Poly Acrylic acid block copolymer using RAFT polymerization

**Kei Kaneko**

**Japan Advanced Institute of Science and Technology**

## 1. Introduction

Recently, polymer nanocomposites have attracted great interests because their properties such as gas permeability, transparency, and mechanical properties are dramatically improved at a low filler loading[1,2]. The most important parameter to control the properties of these materials are related to the dispersion and morphology of inorganic filler. Nano-level dispersion of inorganic filler is essential to achieve the above mentioned improvements. Polystyrene (PS) is one of the most widely used plastics due to its excellent physical properties and low-cost. PS-based nanocomposites have attracted particularly large expectation owing to its high demand in the market. However, it is difficult to achieve good dispersion of filler in PS due to poor compatibility. The most frequently employed methods for overcoming this problem is organic modification of filler surfaces[3]. A new promising approach for preparing better PS nanocomposites is to apply the reverse micelle technique.

Block copolymers react in solvents which are good dissolve property of one block but poor part form micelles. Nanoscale domains which are formed by the block copolymer can provide an area for the growth of the nanoparticles. Shape control of versatile method for the preparation of nanoparticles of size, has attracted a great deal of attention in the literature. Block co-polymer has been proven to be very useful.

Furthermore, the block structure can promote the modification of the nanoparticle surface. Inherently hydrophilic-hydrophobic block copolymers form the micelles in organic solvent.

Generally, block copolymer was synthesized by living polymerization. Which was employed by anionic polymerization.  However, the reaction was difficult to control by sensitive to atmospheric moisture.  We attempted to develop more versatile strategy for the large-scale fabrication of PS-b-Poly Acrylic acid (PAA) block copolymer using RAFT polymerization.  Because of the most important methodologies reported, compatibility with the mild reaction conditions are most promising and likely be reversible addition–fragmentation chain transfer (RAFT) polymerization is raised.  The RAFT polymerization process is shown in Scheme 1.  This is a small amount of will be the introduction of thiocarbonylthio compound as a chain transfer agent in free-radical polymerization system. [4].

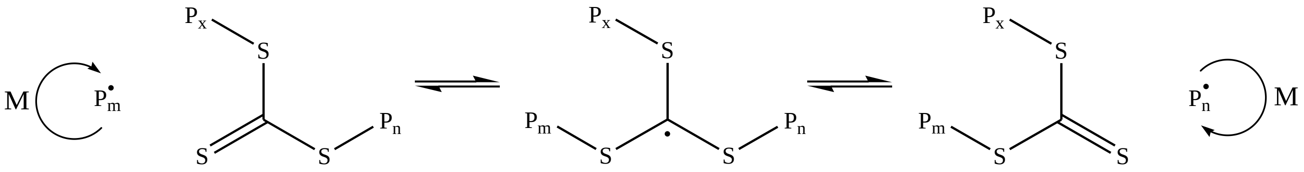

Scheme 1.  Mechanism of chain transfer reaction

## 2. Experimental

### *2.1. Materials*

Benzyl chloride, Carbon disulfide, Potassium carbonate and N,N-Dimethylform amide were used as synthesis of dibenzyl trithio carbonate(DBTTC) (chain-transfer reagent (CTA)). 2,2'-Azobis(isobutyronitrile) was used as a radical initiator. Styrene and acrylic acid were purified by filtration through a neutral alumina, to remove the stabilizer. Tetrahydrofuran (THF) and Methanol were use as solvent.

### *2.2. Synthesis of DBTTC*

Benzyl chloride (2.01 g, 26.2 mmol) and carbon disulfide (3.15 g, 25.0 mmol) added into N,Ndimethylformamide (DMF) (25 mL). Potassium carbonate (K2CO3) (3.45 g, 25.0 mmol) was added intothe solution at 25°C. The mixture was stirred at 40 °C for 24 h. The result was quenched by ice-water. The product was extracted with ethyl acetate. The solution was dried over anhydrous sodium sulfate. Then the mixture was filtered, and evaporated in vacuum. Finally, purification was achieved by silica gel column chromatography with hexane. The result of pure DBTTC was a yellow oil.

### *2.3. Synthesis of Polystyrene*

The typical RAFT agent of DBTTC, solvent, AIBN, and styrene were transferred to flask, degassed by $N_2$ bubbling. The flask were heated at 70 °C for 3, 6, or 12 h. The polymerizations were quenched by ice-water in liquid nitrogen. Samples of the monomer/polymer mixture were dissolve in THF. The polymer was purified by precipitate into methanol. The results of the polymer was shown in Table 1.

The result of PS (Mn: $2.82 \times 10^3$ and $7.192.82 \times 10^3$) was used to macro-CTA for the synthesis of a block copolymer consisting of PS and PAA ([Sty]:[AA]=10:3). The polymerizations were carried for 12 h under a nitrogen atmosphere. The products were purifying by reprecipitation from THF solvents into methanol.

### *2.4. Sample Analyses*

$^1$H and $^{13}$C nuclear magnetic resonance (NMR) spectroscopy measurements were performed using tetramethylsilane as an internal standard at ambient temperatures. The Mw/Mn indices of the polymers were measured on a gel permeation chromatography (GPC) using chloroform.

## 3. Results and Discussion

### *3.1. Synthesis of DBTTC*

The mixture changed to red solution immediately after $CS_2$ addition, indicating the formation of trithiocarbonate anion ($CS_3^{2-}$) [5]. Then, the mixture becomes yellow in color after adding benzyl chloride due to the $CS_3^{2-}$ reacting with benzyl chloride. The suspension was stirred at 40 °C for 24 h. The result was quenched by ice-water. The product was extracted with ethyl acetate. The solution was dried over anhydrous sodium sulfate. Then the mixture was filtered, and evaporated in vacuum. Finally, purification was achieved by silica gel column chromatography with hexane. The result of pure DBTTC was a yellow oil (15 %).

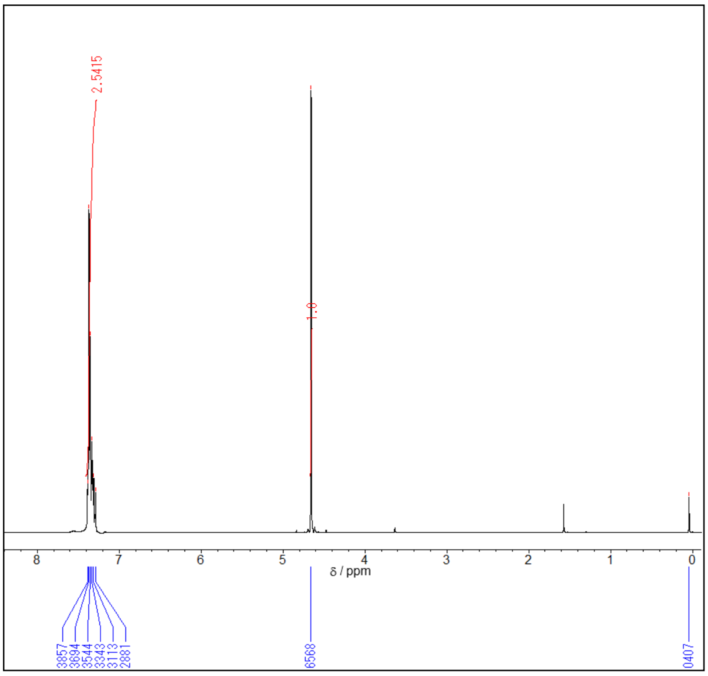

Figure 1. $^{1}H$ NMR spectrum of DBTTC.

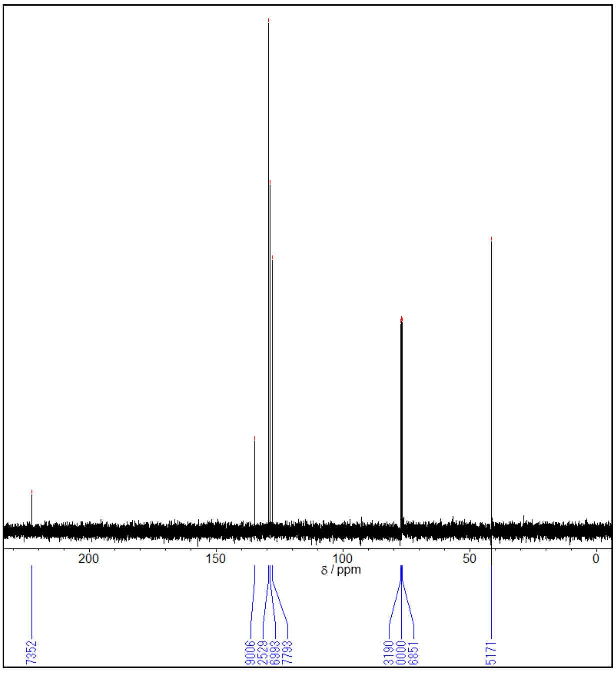

Figure 2. $^{13}C$ NMR spectrum of DBTTC.

The structure analysis of dibenzile tritiocarbonate was examined by NMR (Figure 1, 2). Which were assigned to the S-CH-S bond and phenyl peaks. This implies the formation of the ligand. The DBTTC was determined by $^{1}H$ NMR and $^{13}C$ NMR. The $^{1}H$ NMR spectra of the product show peaks of 4.66 ppm (s, 4H, S-$CH_2$), 7.29–7.39 ppm (10 H, ArH). The $^{13}C$ NMR spectra of the product show peaks of 41.5 ppm ($SCH_2$), 127.7, 128.7, 129.2 ppm, 134.9 ppm ($C_6H_5$), 222.7 ppm (C=S). Therefore, synthesis of

DBTTC can be achieved.

### *3.2. Synthesis of PS*

Table 1. Molecular weights and Mw/Mn of PS samples

| Run | THF(ml) | [Sty]/[CTA]/[AIBN] | Time(h) | Mn x $10^3$(g / mol) | Mw/Mn |
|---|---|---|---|---|---|
| 1 | 0 | 300/0/1 | 12 | 2.11 | 2.16 |
| 2 | 25 | 300/1/1 | 12 | 0.83 | 1.48 |
| 3 | 0 | 300/1/1 | 6 | 1.81 | 1.32 |
| 4 | 0 | 300/1/1 | 9 | 2.73 | 1.36 |
| 5 | 0 | 300/1/1 | 12 | 2.82 | 1.39 |
| 6 | 0 | 1000/1/1 | 6 | 3.73 | 1.45 |
| 7 | 0 | 1000/1/1 | 9 | 6.37 | 1.53 |
| 8 | 0 | 1000/1/1 | 12 | 7.19 | 1.47 |

Table 1 shows the molecular weight and Mw/Mn of synthesized PS. The molecular weight (Mn) of the PS **2** was around 8.3x$10^3$. Because the yield of this polymer was around 15 %, due to the solvent volume was too much and the reaction rate makes slowly. Mw/Mn of the sample **2-8** was less than PS1 with a low degree of polymerization. Figure 2,3 shows a linear relationship between reaction time and Mn of polymerization of PS. First-order reaction kinetics, the concentration of free radicals, has suggested that remained constant during the polymerization. All of these results, RAFT polymerization of DBTTC and PS as transfer agent, has confirmed that it is possible to control the living radical polymerization.

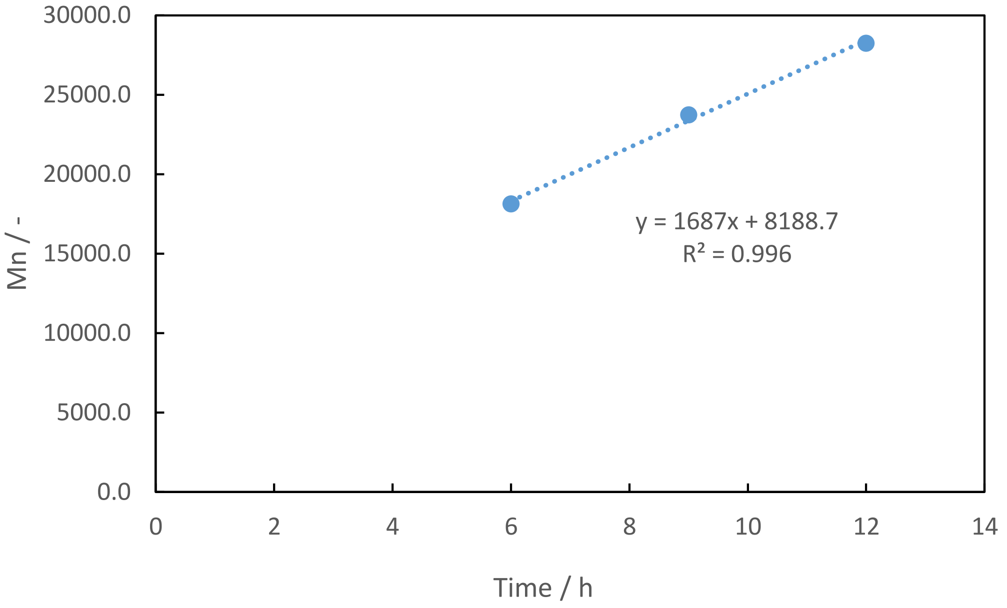

Figure2. Plots of Mn versus the reaction time ([Sty]/[CTA]/[AIBN]=300:1:1)

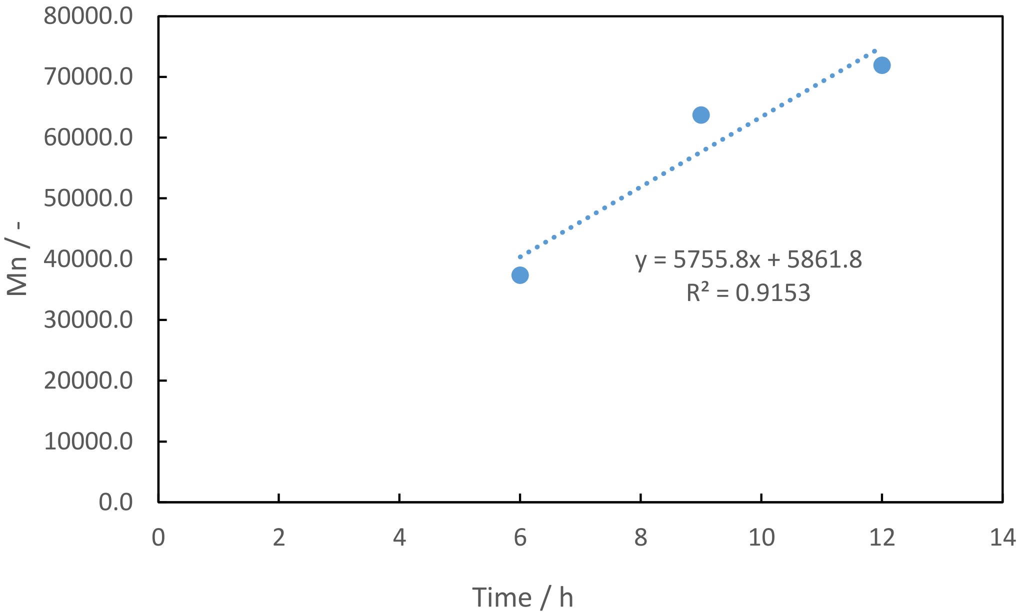

Figure3. Plots of Mn versus the reaction time ([Sty]/[CTA]/[AIBN]=300:1:1)

### *3.3. Synthesis of PS-b-PAA*

Table 2. Molecular weights and Mw/Mn of synthesizes samples

| Run | Mn(PS) x $10^3$(g / mol) | Time(h) | Mn x $10^3$(g / mol) | Mw/Mn |
|---|---|---|---|---|
| 9 | 2.82 | 12 | 1.11 | 1.78 |
| 10 | 7.19 | 12 | 3.48 | 1.70 |

Table 2 shows the molecular weight and Mw/Mn of synthesized polymer. These molecular weights (Mn) of the **9**, **10** were lower than molecular weight of PSs. Because of these synthesized polymers did not dissolve in chloroform. However, these polymers form colloidal liquid in chloroform. It suggested that these polymers build the micelles. Therefore, synthesized polymers may be form block polymer.

## 4. Conclusions

The molecular weight of PS was increased linearly polymerization time. Mw / Mn was still low in the range from 1.32 to 1.53. The molar ratio of experimental parameters [STY]/[CTA], it gave an impact on quite styrene polymerization. RAFT polymerization of styrene has been carried out in the presence of AIBN and DBTTC as respective start and CTA. DBTTC can be easily synthesized and it was found to be good candidates for controlling the polymerization of styrene.

## 5. References

[1] A. Okada, A. Usuki - Macromol. *Mater. Eng.*, **291**, 1449-1476 (2006).

[2] K. Asuka, B. Liu, M. Terano, K. Nitta, Macromol. *Rapid Commun.*, **27**, 910-913 (2006).

[3] L.Zan, S.Wang, W.Fa, Y. Hu, L.Tian, K.Deng, *Polymer* **47** 8155-8162 (2006).

[4] X.Huiliu, G.B. Zhang, X.F.Lu, J.Y.Liu, D.Pan, Y.S.Li, *J. Polym. Sci. A. Polym. chem.*, **44**, 490-498 (2006).

[5] E. Wertheim *J. Am. Chem. Soc.*, **48**, 826-830 (1926)